NTNU
Innovation and Creativity

Robustness Tests and Analysis of Control Strategies on an Electro-pneumatic Actuator

Kristoffer Gjone

Master of Science in Engineering Cybernetics
Submission date: May 2007
Supervisor: Tor Arne Johansen, ITK

Norwegian University of Science and Technology
Department of Engineering Cybernetics

Problem Description

Robustness is very important in safety critical automotive applications, such as clutch actuation. We must thus choose the control strategy giving the best tradeoff between accuracy and robustness. In this project, the student is invited to design and test a sliding mode controller and compare its performance to that of a simple PD controller and an observer backstepping controller. Sliding mode control is interesting because of its robustness when faced with bounded modelling errors. Sliding mode control is also likely to be well suited for the on/off type of control we see when using on/off pneumatic valves to control the actuator.

Assignment given: 08. January 2007
Supervisor: Tor Arne Johansen, ITK

PREFACE

The work leading to this thesis was carried out between January and June, 2007 at the Norwegian University of Science and Technology (NTNU). The problem considered in this thesis has been formulated by the R&D group on clutch actuation systems at Kongsberg Automotive ASA, and I would like to thank Sten Roar Snare and Christian Bratli for lots of guidance and feedback during my work with the thesis. I would also like to thank Tor Arne Johansen at NTNU.

Through the work on this thesis I have been able to go through all the stages of a controller design project, from problem formulation, through design and simulations and finally in experimental tests at KA. This has provided me with useful insights that I did not have before i started the work on this master's thesis. I hope this experience will be helpful in future work situations.

Trondheim, May 31, 2007

Kristoffer Gjone

CONTENTS

SUMMARY

In this thesis a Sliding Mode Controller (SMC) is designed for an electro-pneumatic clutch actuator controlled by two on/off valves with PWM. The areas of application of the clutch actuator is in Automated Manual Transmission (AMT) and Clutch-by-wire (CBW) systems in heavy-duty trucks. As with most automated systems in the automation industry safety is the main priority, and in a cybernetic point of view this means that robustness of the control systems is very important. Sliding Mode Controllers are known for their excellent robustness properties and the focus of this thesis is to validate these properties for this particular application.

The robustness properties of the SMC also indicates that a simple design model is adequate and since the existing mathematical models for this system are quite complex some simplifications are introduced.

The controller design is performed in two phases. First an ideal SMC is designed, but since this introduces discontinuities in the control law any practical implementation would give heavy chattering at the output from the controller. Therefore a continuous linear approximation to the discontinuity is introduced. This controller is known as a *boundary layer controller* and it will reduce the control chattering to an acceptable level. The ideal controller is proven to be asymptotically stable, while for the boundary layer controller ultimate boundedness is achieved and a linearisation is performed for the case of a constant reference and this analysis shows that the origin of the linearised system is a stable focus. This indicates that the boundary layer controller might also be asymptotically stable.

Since only a position measurement is available to the control system the rest of the system states must be estimated. Velocity and acceleration are simply estimated as the first and second order filtered derivatives of the position measurement. The pressure is estimated based on the equation of motion for the clutch actuator.

Through computer simulations and experimental testing the SMC has shown satisfying tracking performance and very good robustness with respect to parameter variations. Comparisons with a PD and a Backstepping controller shows that the performance of the SMC is superior to the PD controller and absolutely comparable to the Backstepping controller, though they have different strengths and weaknesses and therefore yield rather different results.

CHAPTER 1

INTRODUCTION

In this chapter an introduction to the system considered in this thesis is presented, along with some background information supporting the need for a robust control system for clutch actuation. A short problem formulation is also presented to concretise the goals of this thesis. Last an outline of the organization of this thesis is presented.

1.1 BACKGROUND

In recent years Automated Manual Transmission systems (AMT) have attracted more and more attention from the automotive industry since they combine the best properties of manual and automatic transmissions. Manual transmissions are lighter and have considerably less power loss than conventional automatic transmissions. However, many drivers still prefer automatic transmissions because of their convenience especially in city traffic with frequent starts and stops. This is also the case for many professional drivers who typically drive heavy duty trucks where the power losses suffered from a conventional automatic transmissions means a considerably higher fuel consumption and hence less profit and are in practice not an option. Therefore AMT systems in heavy duty trucks are of special interest.

In a passenger car, the AMT system is often implemented using hydraulic units for clutch engagement. In most trucks pressurized air is available and therefore a pneumatic actuator will be a less expensive solution than a hydraulic one. Another advantage of pneumatics over hydraulics is a simpler maintenance and a more environmentally friendly solution because of the danger of leakage from a hydraulic system. However pneumatic actuators are inherently difficult to control because of significant nonlinearities in the models, mainly due to the compressibility of air. Combined with a highly nonlinear characteristic of most clutch compression springs used in heavy duty trucks, the pneumatic actuators makes the electro-pneumatic clutch actuator a difficult system to control.

In (Kaasa, 2003) an observer backstepping controller was designed, and it was extended to an adaptive backstepping controller by Lokken (2006). The major drawback of the backstepping control technique is that it is based on cancellation of undesirable nonlinearities in the system and therefore depends heavily on good mathematical models and

good parameter estimates to give high performance. For the electro-pneumatic clutch actuator the mathematical models are well known, but the full models are too complex to be used in controller design. Combined with parameter variations due to mechanical wear and tear on the clutch, this requires the controller to be very robust.

Another ”problem” with the backstepping controllers which have been designed by Kaasa (2003) and Lokken (2006) is that they require the full state vector to be available. Since, because of economic and maintenance considerations the position is the only measurement available to the control system a full state observer has been designed by Kaasa (2003) and has been extended to an adaptive observer by Vallevik (2006). There are mainly two problems with the use of an observer in the control system. Firstly the complexity of the mathematical model and the parameter uncertainty are causes of estimation error in the observer. Especially, as discussed by Vallevik (2006) the friction modelling is the major problem in the observer design. The second problem with the use of an observer is that in a commercial implementation of the system it is desirable to use 10ms sample time instead of 2ms which is often used in the test lab.

1.2 System Description

The clutch actuation system used in this thesis is almost identical to the system described in (Kaasa, 2003), (Lokken, 2006) and (Vallevik, 2006). The major difference is the use of On/Off valves in this thesis instead of the three way proportional valve. In Figure 1.1 a schematic drawing of the system is presented. The main parts of the system are a friction clutch, a pneumatic actuator, two on/off-valves, a control system and a position sensor. A more detailed description is given below:

Friction clutch: The purpose of the clutch is to allow the driver of the car to disengage the engine from the rest of the drive line. The friction clutch consists of two friction plates and a diaphragm spring that push the plates together when no input is given to the system. When the plates are pulled away from each other less and less torque is transferred from the engine to the drive line, and when fully disengaged no torque is transferred. This is required during start and stop and during a gear change.

Pneumatic actuator: The pneumatic actuator is connected to the clutch spring and can therefore be used to control the torque that is transferred from the engine.

Valves: Two on/off-valves are used to control the flow of air in and out of the chamber in the pneumatic cylinder.

Control system: The control system uses the measurement of the position of the piston

in a feedback controller to control the air flow rate into the chamber and therefore the position of the clutch. It is implemented on a digital computer.

Position sensor: The only measurement in the system is a position sensor that is used to measure the position of the piston and transmit the value to the control system.

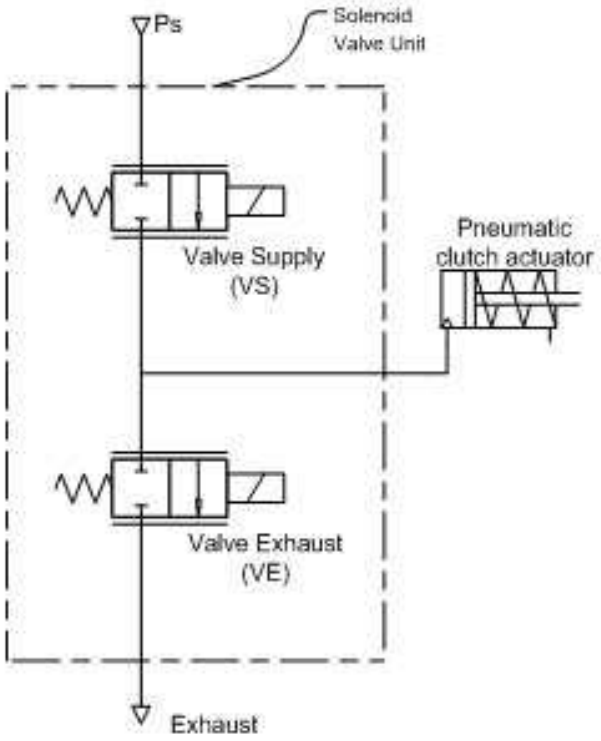

Figure 1.1: Clutch system overview

1.3 PROBLEM FORMULATION

Robustness is very important in safety critical automotive applications, such as clutch actuation. The control strategy must therefore be chosen to give the best tradeoff between accuracy and robustness. Sliding Mode Controllers have shown great robustness, disturbance rejection and need only limited knowledge of the system to be controlled, and should be well suited for this application.

Therfore the goal of this thesis is to design an SMC for the system described in Section 1.2. The focus for the computer simulations and the experimental tests of the controller will be to check the robustness properties and to compare the SMC to a simple PD-controller and a Backstepping controller, since these are already implemented for the clutch actuator.

1.4 THESIS OUTLINE

This thesis is organized in the following chapters:

Chapter 2: A literature review of some existing work and theory on sliding mode control.

Chapter 3: Descriptions of the mathematical models used for computer simulations and controller design.

Chapter 4: Design and stability analysis of the sliding mode controller.

Chapter 5: Extensions to the controller designed in Chapter 4. The extensions include a pressure estimator, extended friction modelling and a controller with integral effect. The chapter also include analysis of the effects of the controller extensions.

Chapter 6: Results from computer simulations of the sliding mode controller. The focus of the tests are the robustness properties of the controller. The chapter also contains some comments of the results obtained.

Chapter 7: Experimental results from test rig and car performed at Kongsberg Automotive. Both a robustness test much like the computer simulations and a comparison with a backstepping controller and a PD controller are presented. Comments of the results are also presented.

Chapter 8: Discussions of the results obtained through computer simulations and experiments. Also includes some concluding remarks concerning the use of Sliding mode control in the electro-pneumatic clutch actuator and some recommendations for future work that should be considered.

Appendix A: Presents mathematical results and proofs which have been considered to be to detailed to include in the text of the thesis.

Appendix B: Some figures and plots from simulations and experiments.

CHAPTER 2

LITERATURE REVIEW

In this chapter a short review of existing work on control of electro-pneumatic actuators is presented along with some background theory concerning variable structure control (VSC) with special focus on VSC systems with Sliding Mode Control (SMC). A simple design example for an SMC is also presented to illustrate the basic concepts of the design procedure and the stability analysis of such controllers.

2.1 CONTROL OF ELECTRO-PNEUMATIC ACTUATORS

As discussed by Kaasa (2003) many different control design approaches has been applied to position tracking of electro-pneumatic actuators. In the following a short presentation of the most important contributions to solving this control problem is presented. To structure the presentation the design approaches are grouped in three different categories: Linear control, Feedback linearisation and Sliding mode control.

2.1.1 LINEAR CONTROL

Since pneumatic actuators have inherent low stiffness and low damping, PD-controllers have generally shown poor performance when applied to electro-pneumatic actuators. Therefore different approaches have been proposed when designing linear controllers for these systems. As Kaasa (2003) describes most of these approaches are based on the following 3rd-order normal form model (i.e. a forced mass-spring-damper system)

$$\frac{d}{dt}\begin{bmatrix} y \\ \dot{y} \\ \ddot{y} \end{bmatrix} = \begin{bmatrix} 0 & 1 & 0 \\ 0 & 0 & 1 \\ 0 & -\omega_n^2 & -2\zeta_n\omega_n \end{bmatrix}\begin{bmatrix} y \\ \dot{y} \\ \ddot{y} \end{bmatrix} + \begin{bmatrix} 0 \\ 0 \\ K\omega_n^2 \end{bmatrix} u \tag{2.1}$$

where y is defined as a deviation from an equilibrium point y^*. K is the steady-state gain, ω_n is the resonance frequency and ζ_n is the damping coefficient. The inherent difficulties of controlling pneumatic actuators are caused by low values for both ω_n and ζ_n and the fact that both those parameters vary significantly as a function of y.

Given the model (2.1) the resulting linear control law will be

$$u = -K_p(y - y_r) - K_v\dot{y} - K_a\ddot{y} \tag{2.2}$$

where y_r is the desired reference, and K_p, K_v and K_a are the controller gains. The feedback gains can be calculated in different ways using a variety of different techniques, e.g. pole placement and steady-state linear quadratic optimal control etc. The application of the control law in (2.2) among with experimental results can be found in (Virvalo, 1995), (J.Wang et al., 1999) and (X.Brun et al., 1999).

The controller in (2.2) requires a full-state feedback including position, velocity and acceleration. In the literature the two most common approaches are using filtered numerical differentiation or an observer approach. Most popular is the numerical differentiation mostly due to its simplicity, but a major drawback of this approach is high susceptibility to measurement noise particularly in the 2nd-order derivative. Another approach is a state observer, and the most common observer for this purpose is the Luenberger-observer, either a full-order or reduced-order observer. Both the observer and the differentiation approach is investigated by Virvalo (1995).

To avoid the need for a full-state feedback an approach based on discretization of the system equation and the use of dynamic output feedback control has been proposed by Shih and Huang (1992) and Virvalo (1995).

2.1.2 Feedback linearisation

Since the models of pneumatic actuator systems contain significant nonlinearities, the interest of research communities eventually turned to nonlinear control design techniques. The first pure nonlinear tracking controller applied to electro-pneumatic actuators was an *input-output feedback linearising controller*, in (E.Richard and S.Scavarda, 1989). The basis for the controller design was a 4th-order nonlinear model as presented by Kaasa (2003). The use of a feedback linearising controller requires the nonlinearities of the model to be differentiable which was particularly restricting on the friction modelling since many friction models contain discontinuities. In most of the appliances of this control design technique a pure viscous friction model was used, i.e. $f_f(v) = Dv$. Despite the limitations of the models used this control design approach, superior tracking performance was achieved compared to linear controllers. The major drawback of this approach is that the cancellation of nonlinearities gives the controller poor robustness properties, which can be very important in many applications of pneumatic actuators.

As an alternative to the method presented above F.Xiang and J.Wikander (2004) presents what is called a *Block-oriented approximate feedback linearisation*. The use of approximate cancellation allow the use of non-smooth nonlinearities, e.g. discontinuous friction models. Another alternative to the straight forward input-output feedback linearisation

presented by E.Richard and S.Scavarda (1989), an *input-state feedback linearisation* is considered by Kimura et al. (1997).

2.1.3 Sliding mode control

Sliding mode control is known to yield very good robustness properties and is one of the most popular approaches to nonlinear tracking control of electro-pneumatic actuator. Since this design technique is presented in detail later in this chapter, only a presentation of the previous work in the are is presented here. In (Bouri et al., 1994) and (T.Acarman et al., 2001) sliding mode controllers based on the 4th-order model that was used in most feedback linearizing approaches as described earlier. The inherent robustness to modelling errors of sliding mode controllers has inspired design approaches based on simplified 3rd-order models where the pressure states has been replaced by one single pressure state. Designs based on this model is presented by Pandian et al. (1997a) and further extended to an adaptive design in (Pandian et al., 1997b). Paul et al. (1994) proposes the use of a reduced order sliding mode controller. In recent years *higher order sliding modes* has been developed and it has been applied to electro-pneumatic actuators in (Laghrouche et al., 2004, Lagrouch et al., 2006).

2.2 A brief history of VSC

Variable Structure Control (VSC) with sliding mode control was a concept first developed by Emelyanov and his fellow researchers in the Soviet Union in the early 1950's. As described by Hung et al. (1993) the development of VSC can be divided into three phases

1. *The early stage (1957-1970)*: The VSC systems studied were linear systems with a single input, the switching surface had a particular quadratic form and the control law was a simple relay controller.

2. *VSC for Multi-Input Linear Systems (1970-1980)*: In this period the theory of VSC was extended to linear systems with multiple inputs. Still VSC did not gain too many supporters. The main reasons being the popularity of linear control system designs and the fact that the full robustness potential of VSCs was not recognized yet.

3. *State of the art VSC development (1980-present)*: In this period the VSC design technique was generalized to include a wide range of system models such as nonlinear systems, discrete-time systems etc. VSC theory was also developed for several control objectives including tracking, model following and state observation.

Also the impressive robustness properties of VSC was fully recognized during this period leading to more interest from the general research community. Applications in a variety of engineering challenges also helped the VSC technique's popularity.

The development of Variable Structure Control is still an active field of research and one of the most promising developments in recent years is the discovery of Higher-Order Sliding Modes as described by e.g. Levant (2003). This technique promises to solve the problem of chattering, which is the most important problem in practically implemented VSC systems while preserving the robustness features.

2.3 IDEAL SLIDING MODE CONTROLLER DESIGN

As described by Utkin (1977) the basic concept of VSCs is that the system is allowed to change structure at any instant. The design problem in VSCs is therefore to find the parameters in each of the system structures and to design the switching logic which decide when the structure of the system should change. One of the key features of Variable Structure Systems is that the resulting system can show properties not present in any of the separate system structures. For instance a desired trajectory in the phase plane can be constructed from parts of the trajectories of the separate structures. The motion described by these trajectories is known as *sliding mode*.

The response of a system with sliding mode control can basically be divided into two parts

1. *The reaching phase*: When $s \neq 0$, the system is said to be in the reaching phase. The trajectories in the phase plane will in this phase move toward S.

2. *The sliding phase*: Once the system reaches S the trajectories will move along the surface described by S until it reaches the equilibrium point.

To illustrate some of the concepts and properties of the VSC with sliding mode control mentioned earlier in this chapter a simple example is introduced where a second-order non-linear system is used as the plant for the control design.

Considering the second order system

$$\begin{aligned} \dot{x_1} &= x_2 \\ \dot{x_2} &= f(x) + g(x)u + \delta(t) \end{aligned} \tag{2.3}$$

where $f(x)$ and $g(x)$ are known (generally nonlinear) functions and $\delta(t)$ represents any bounded uncertainties, such as modeling imperfections and bounded disturbances. The

sliding manifold, S could e.g. be defined by $s(x) = x_2 + a_1 x_1 = 0$. This yields the following system behavior once the system has reached the manifold

$$x_2 = -a_1 x_1 \quad \Rightarrow \quad \dot{x_1} = -a_1 x_1$$

which implies that both x_1 and x_2 converges exponentially to zero.

The next step is to define a control law that ensures that the sliding manifold is reached in finite time and remains there for all future time. First the time derivative of the sliding function $s(x)$ is found to be

$$\dot{s} = a_1 x_2 + \dot{x_2} = a_1 x_2 + f(x) + g(x)u + \delta(t)$$

Suppose that $\delta(t)$ satisfies the inequality $|\delta| \leq D$ By defining the Lyapunov-like function[1] candidate $V = \frac{1}{2}s^2$ we have

$$\begin{aligned} \dot{V} &= s\dot{s} \\ &= s[a_1 x_2 + f(x)] + s\delta(t) + g(x)su \\ &\leq s[a_1 x_2 + f(x)] + |s|D + g(x)su \end{aligned} \tag{2.4}$$

Now, u needs to be designed to ensure that $\dot{V}$ is negative definite. One controller that yields $\dot{V} \leq 0$ is

$$u = u_{eq} - k \cdot sign(s) \tag{2.5}$$

where $k = \frac{D+c}{g_0}$, where $c > 0$ and $g(x) \geq g_0 \geq 0$. u_{eq} is known as the equivalent control law and is designed to cancel all known nonlinearities in the system under ideal conditions. $sign(\cdot)$ is defined as

$$sign(x) = \begin{cases} 1, & x > 0 \\ 0, & x = 0 \\ -1, & x < 0 \end{cases}$$

For the system in this example

$$u_{eq} = \frac{-f(x) - a_1 x_2}{g(x)} \tag{2.6}$$

The control law (2.5) yields

$$\dot{V} \leq -c|s|$$

Then by defining $W = \sqrt{2V} = |s|$ we have that the upper right-hand derivative D^+W satisfies the inequality

$$D^+W \leq -c, \ \forall \ |s(t)| > 0 \tag{2.7}$$

[1] $V(s)$ is only a *Lyapunov-like* function since it is a function of s, and not of x directly

Combining the result from (2.7) with the Comparison Lemma (Khalil, 2000, Chap. 3) yields

$$|s(t)| \leq |s(0)| - ct, \ \forall \ |s(t)| > 0$$

This means that all trajectories of the system reaches the sliding manifold S in finite time and will remain there for all future time.

Figure 2.1 shows the responses of the ideal controller with $f(x) = x_1^2 + sin(x_2)$ and $\delta(t) = sin(t)$. The controller constants were chosen to be $a_1 = 5$ and $k = 50$. The last plot in Figure 2.1 clearly illustrates the reaching phase and the sliding phase. Although the plot of x_1 shows a good response the plot of u illustrates one of the major drawbacks of variable structure control systems, namely chattering. Methods of overcoming this problem is discussed in the remainder of this chapter.

2.4 CHATTERING

One important drawback of the ideal sliding mode controller in 2.5 is that it leads to a discontinuous control law which in any practical implementation of the controller will result in a phenomenon known as chattering[2]. As described by Young (2002) there are two mechanisms that produce chattering:

- The ideal switching required to implement the controller in 2.5 implies an infinite switching frequency that is impossible to achieve in a practical implementation of the controller.
- Parasitic dynamics in sensors and actuators that produce a low amplitude, high-frequency oscillation in the neighborhood of the switching manifold.

2.4.1 CHATTERING HANDLING

Since chattering is the most significant problem in practical implementations of sliding mode controllers, chattering handling has become an important part of the controller design. In the litterature several techniques has been proposed to overcome the problem, and some of them are presented here. As described by both Khalil (2000) and Slotine and Li (1991), the most common approach to remove the chattering when implementing an SMC is known as *boundary layer control*. The chattering problem is overcome by smoothing out the control discontinuity in a boundary layer around the manifold, *S(t)*. This technique is described in more detail later in this chapter.

[2]Chattering in a control system is defined as high frequency oscillations of the control signal

In (Hung, 1993) two alternative methods for chattering avoidance are described. The first technique is based on a augmentation of the plant to be controlled. The basic idea of this method is to introduce a first-order "augmenting network" between the output of the controller and the input of the plant, thereby removing the chattering at the input to the physical plant. Next a Fuzzy Adaptive scheme is described, where an estimate of the perturbation assumed to enter at the plant input and a fuzzy decision maker is combined to make the magnitude of the signum term in the controller adaptive.

The most recent results concerning chattering handling is the development of the theory concerning Higher-order sliding modes described by Levant (2003) and Dynamic sliding mode (Koshkouei et al., 2005). This technique promises to completely remove the chattering and still preserve the excellent robustness qualities of Sliding Mode Control.

2.4.2 Boundary Layer Control

The boundary layer is used to smooth out the discontinuous control is defined as

$$B = \{x, |s(x)| \leq \epsilon\}, \quad \epsilon > 0$$

In practice this is done by replacing the signum function in (2.5) with a saturation function. This yields

$$u = u_{eq} - k \cdot sat(\frac{s}{\epsilon}) \tag{2.8}$$

where ϵ is known as the boundary layer thickness, and the saturation function is defined as

$$sat(y) = \begin{cases} y, & if\ |y| \leq 1 \\ sign(y), & if\ |y| > 1 \end{cases}$$

For the system in (2.3) the boundary layer controller will ensure that all trajectories will converge to the set $\Omega_\epsilon = \left\{ |x_1| \leq \frac{\epsilon}{a_1},\ |s| \leq \epsilon \right\}$. The behavior inside the set Ω_ϵ is problem dependent and requires a more rigorous stability analysis and good knowledge of the dynamics of the system.

Figure 2.2 shows the responses of the boundary layer controller with the same example system that was used to test the ideal sliding mode controller. The plots clearly show a response very similar to that of the ideal sliding mode controller, but without any chattering.

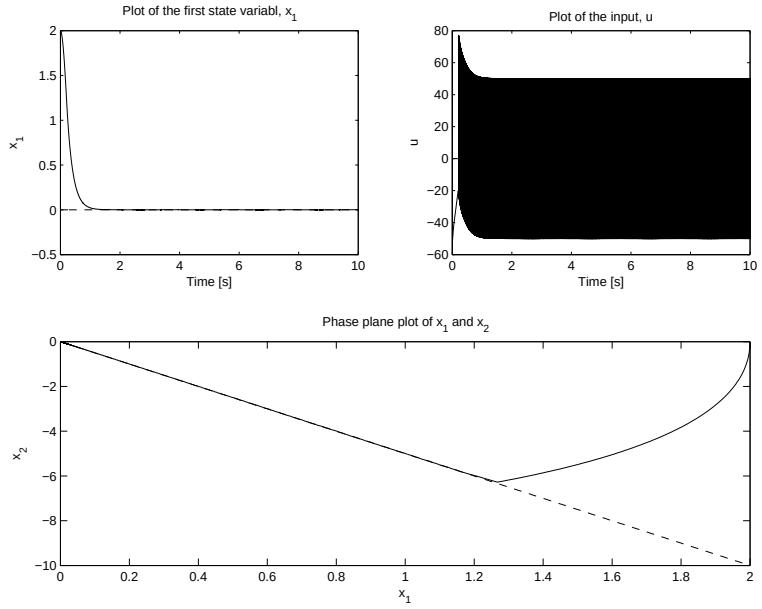

Figure 2.1: Plot of x_1, u and phase plane plot for the ideal sliding mode controller. The dotted line in the phase plane plot is the sliding surface S.

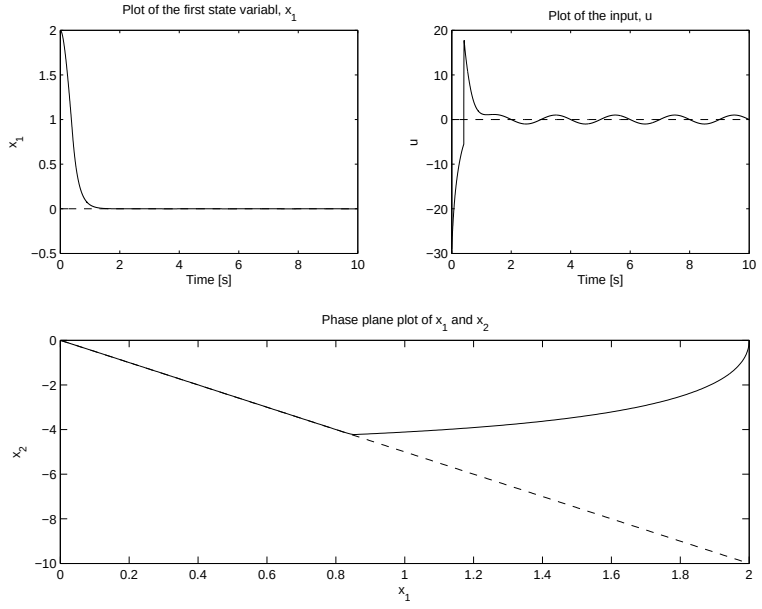

Figure 2.2: Plot of x_1, u and phase plane plot for the boundary layer sliding mode controller. The dotted line in the phase plane plot is the sliding surface S.

2.4.3 Limitations of the boundary layer technique

Although the boundary layer approach to constructing a practical sliding mode controller looks very promising at first, mainly because of its simplicity, there are many limitations that prevent it from being the optimal solution to the chattering problem. As Young (2002) points out, the piecewise linear approximation of the switching control actually reduces the closed loop system into a system without sliding mode. Another important limitation of this technique is that it compromises the robustness and disturbance rejection properties that are actually the biggest strengths of Sliding Mode Controllers.

CHAPTER 3

MATHEMATICAL MODELS

In most control design techniques mathematical models play a crucial role. The most obvious area of application is as a basis for the controller design. In most classic, linear design techniques (e.g. PID controllers) the model is often used to assist the tuning of the controller gains, for stability analysis and for performance evaluations. Modern, nonlinear design techniques (Sliding mode control, Backstepping, etc.) often use the model more directly to cancel out known nonlinearities in the system to achieve better performance and improve the stability of the controller. These techniques often require a more accurate model than the classic ones, as parts of the model is used directly in the feedback. Another important area of application of mathematical model is in computer simulations to verify the properties and performance of the controller. This is important both during the design phase to check the validity of what has been done so far and is also a useful tool for documenting the performance and stability of the controller.

An important aspect in mathematical modeling for controller design purposes is also the need for different models in various areas of application. For instance the model used for computer simulations should generally be very accurate to mimic the behavior of the real physical system as accurately as possibly, while this model is often too detailed and complex to be used as basis for a controller design. Therefor several mathematical model of the clutch actuation system is presented in this chapter.

3.1 SIMULATION MODEL

The model that will be referred to as the simulation model in this thesis is the model derived by Kaasa (2003). Since this is a very detailed model of the physical system it is used to test and validate the controller before any experimental testing is done. A short description of the model will be provided in this section.

To derive the motion dynamics of the clutch actuation system, Newton's Second law is applied to the actuator piston

$$\dot{y} = v \tag{3.1}$$

$$\dot{v} = \frac{A_A}{M} p_A - \frac{A_B}{M} p_B - \frac{1}{M} f_f(v, p_A, p_b, y_f) - \frac{1}{M} f_l(y) \tag{3.2}$$

where y is the position of the actuator piston and v is the velocity. A_A and A_B are the areas of the pistons in the two chambers. p_A and p_B are the pressures in chamber A and B respectively. M is the total mass of the piston. f_f is an expression for the friction force acting on the piston and f_l describes the clutch load characteristic.

The load characteristic is a nonlinear function of the clutch position and is modelled by a parameter affine model using gaussian basis function as

$$f_l(y) = \phi_l^T(y)\Theta_l \tag{3.3}$$

where ϕ_l^T is a vector of basis functions and Θ_l is a parameter vector. The friction force, $f_f(v, p_A, p_b, y_f)$ is based on a two regime Elastoplastic friction model, but will not be discussed further in this thesis.

The model for the pressure and temperature in chambers A and B can be found in Appendix A.1 together with the equations for the air flow in and out of the two chambers. In Appendix refsubsec:simmodparam the parameters and constants used in the simulation model is also presented.

3.2 Full design model

The model described in Section 3.1 is to complex to be used in a controller design and therefore a simplified design model was derived by Lokken (2006)

$$\begin{aligned}
\dot{y} &= v \\
M\dot{v} &= -f_l(y) - f_f(v, y_f) + A[p - P_0] \\
\dot{p} &= \frac{1}{V(y)}(-Avp + RT_0\omega) \\
\tau_v\dot{\omega} &= -\omega + q_v(p, u_v) \\
\dot{y}_f &= g_f(v, y_f)
\end{aligned} \tag{3.4}$$

where y is the position of the clutch, v is the velocity, p is the pressure in chamber A, ω is an expression for the mass flow rate in and out of chamber A and y_f is the pre-sliding deflection used in the LuGre friction model. The constants A,R and T_0 are the area of the actuator piston, the gas constant and the reference temperature respectively. $f_l(y)$ represents the load characteristic of the clutch while $f_f(v, y_f)$ is the friction force. The friction forces in the system are modeled using the LuGre friction model:

$$f_f(v, y_f) = D_v v + K_f y_f + D_f g_f(v, y_f) \tag{3.5}$$

$$g_f(v, y_f) = v - \frac{K_f}{F_d}|v|y_f \tag{3.6}$$

where D_v, D_f and K_f are friction coefficients. To achieve a continuous derivative of $g_f(v, y_f)$, the absolute value is replaced by a smoothed approximation

$$|v| = |v|_s = \sqrt{v^2 + \delta^2} \tag{3.7}$$

where $\delta > 0$ is arbitrarily small. The volume of the actuator is

$$V(y) = V_0 + Ay \tag{3.8}$$

Here V_0 is the dead volume when y = 0[mm]. The function $q_v(p, u_v)$ describes the flow through the valves, and u_v is the control input to the valves. The flow function $q_v(p, u_v)$ is constructed on basis of the valves chosen in the physical implementation.

3.3 Simplified design model

Since a Sliding Mode Controller does not depend heavily on an accurate system model, a simplified design model was derived. The main purpose of the simplification was to reduce the relative degree of the system from 4 to 3. In the context of SMC design, this implies that only the 1^{st} and 2^{nd} derivatives of the output need to be known. The following simplifications was made to the model in (3.4)

Assumption 3.1. *Only viscous friction is considered, giving* $f_f(v, y_f) = f_f(v) = Dv$

Assumption 3.2. *No valve dynamics, giving* $\omega = q_v(p, u_v)$*. This means that* ω *can be considered as the input to the system since* $q_v(p, u_v)$ *can be computed through an inverse flow model.*

This yields the following simplified design model

$$\begin{aligned} \dot{y} &= v \\ M\dot{v} &= -f_l(y) - f_f(v) + A[p - P_0] \\ \dot{p} &= \frac{1}{V(y)}(-Avp + RT_0\omega) \end{aligned} \tag{3.9}$$

where ω is considered as the input variable. The function $f_l(y)$ is defined as

$$f_l(y) = K_l(1 - e^{-L_l y}) - M_l y \tag{3.10}$$

In a more standard form the system in (3.9) can be re-written as

$$\dot{\mathbf{x}} = f(\mathbf{x}) + g(\mathbf{x})u \tag{3.11}$$

$$\begin{bmatrix} \dot{y} \\ \dot{v} \\ \dot{p} \end{bmatrix} = \begin{bmatrix} v \\ \frac{1}{M}[-f_l(y) - f_f(v) + A(p - P_0)] \\ \frac{-A}{V(y)}vp \end{bmatrix} + \begin{bmatrix} 0 \\ 0 \\ \frac{RT_0}{V(y)} \end{bmatrix} u \tag{3.12}$$

with the state vector $\mathbf{x} = [y\ v\ p]$ and the input variable $u = \omega$.

3.3.1 NORMAL FORM

To achieve a system structure that can be used to design a sliding mode controller the system in (3.9) is transformed to the *normal form* as given in (Khalil, 2000)

$$\begin{bmatrix} \eta \\ --- \\ \xi \end{bmatrix} = \begin{bmatrix} \phi(x) \\ --- \\ \psi(x) \end{bmatrix} = \begin{bmatrix} \phi_1(x) \\ \vdots \\ \phi_{n-\rho}(x) \\ --- \\ h(x) \\ \vdots \\ L_f^{\rho-1}h(x) \end{bmatrix} = T(x)$$

where ϕ satisfy the equations

$$\frac{\delta\phi_1}{\delta x}g(x) = 0, \quad \text{for } 1 \leq i \leq n-\rho,\ \forall x \in D$$

For the simplified design model, the normal form representation yields

$$\begin{aligned} \dot{\xi_1} &= \xi_2 \\ \dot{\xi_2} &= \xi_3 \\ \dot{\xi_3} &= f(\boldsymbol{\xi}) + g(\boldsymbol{\xi})u \end{aligned} \tag{3.13}$$

The expressions for $f(\boldsymbol{\xi})$ and $g(\boldsymbol{\xi})$ can be found in A.2.1.

3.3.2 TRACKING MODEL

Since the goal of this thesis is to design a tracking controller for the clutch actuation system, the following model is introduced

$$R = \begin{bmatrix} r \\ \dot{r} \\ \ddot{r} \end{bmatrix},\ \mathbf{e} = \begin{bmatrix} \xi_1 - r \\ \xi_2 - \dot{r} \\ \xi_3 - \ddot{r} \end{bmatrix} = \xi - R$$

The change of variables $\mathbf{e} = \xi - R$ yields

$$\begin{aligned} \dot{e_1} &= e_2 \\ \dot{e_2} &= e_3 \\ \dot{e_3} &= f(\boldsymbol{\xi}) + g(\boldsymbol{\xi})u - \dddot{r} \end{aligned} \tag{3.14}$$

Now the tracking control objective $y = y_d$ can be achieved by designing a controller which ensures that $e(t)$ is bounded and converges to zero.

3.4 LOAD CHARACTERISTICS

The model for the load characteristic that is used in the simple model is given in (3.10) and the parameters are found using a least-squares curve fitting using the function *lsqcurvefit* in MatLab. The data for the curve fitting are found using the load characteristic model based on gaussian basis functions as described in (3.3). To test the robustness of the controller with respect to errors in the load model three different sets of parameters were found, based on three different data sets from the gaussian load model. The three data sets used were the nominal values and $\pm 1000N$ from the nominal values. The corresponding parameters for the simple load model are found in Table 3.4.

	Nominal	**-1000N**	**+1000N**
K_l	3599	3289	3860
L_l	210	191	233
M_l	25105	23092	24747

Table 3.1: Parameters for load model

CHAPTER 4

CONTROLLER DESIGN

The goal of this chapter is to design a robust controller for the electro-pneumatic clutch actuator by using Sliding Mode Control. SMCs are known to be robust to parameter variations and modeling errors.

4.1 IDEAL SLIDING MODE CONTROLLER

The Sliding Mode Controller has been based on the simplified control model given in (3.9). The design process is the same as described in Chapter 2.

4.1.1 SLIDING SURFACE

The sliding surface $S \in \mathbf{R}^{(n)}$ is defined by the scalar equation $s(\mathbf{e}) = 0$, where

$$s(\mathbf{e}) = a_1 e_1 + a_2 e_2 + \cdots + a_{\rho-1} e_{(\rho-1)} + e_\rho$$

and $a_1, \ldots, a_{\rho-1}$ are strictly positive constants and ρ is the relative degree of the system. Since the model in (3.9) has a relative degree $\rho = 3$, $s(\mathbf{e}, t)$ is given as

$$s(\mathbf{e}, t) = a_1 e_1 + a_2 e_2 + e_3 \tag{4.1}$$

If a control law can be designed to drive the system to the sliding surface and maintain it there for all future time (i.e. $s(\mathbf{e}) = 0$) the motion of the system is governed by

$$e_3 = -a_2 e_2 - a_1 e_1 \tag{4.2}$$

since $a_1, a_2 > 0$, (4.2) implies that $e(t)$ converges to zero as t tends to infinity, and the rate of convergence can be controlled by choice of a_1 and a_2.

4.1.2 CONTROLLER DESIGN AND STABILITY ANALYSIS

Given the result from (4.2) the goal of the controller is to bring the trajectory to the surface S in finite time and maintain it there for all future time. The sliding variable $s(\mathbf{e})$ satisfies the equation

$$\begin{aligned} \dot{s} &= \dot{e_3} + a_2 e_3 + a_1 e_2 \\ \dot{s} &= f(\boldsymbol{\xi}) + g(\boldsymbol{\xi}) u - \dddot{r} + a_2 e_3 + a_1 e_2 \end{aligned} \tag{4.3}$$

Considering the Lyapunov-like function candidate $V(s) = \frac{1}{2}s^2$, which satisfies the following conditions

$$\begin{aligned} i)\ & V(s) > 0,\ \forall s \neq 0 \\ ii)\ & V(s) = 0,\ s = 0 \\ iii)\ & V(s) \to \infty,\ \|s\| \to \infty \end{aligned}$$

and the differential equation

$$\begin{aligned} \dot{V} &= s\dot{s} \\ &= s[f(\boldsymbol{\xi}) + a_2 e_3 + a_1 e_2 - \dddot{r} + g(\boldsymbol{\xi})u] \end{aligned}$$

by choosing

$$u = u_{eq} - k \cdot sign(s) \tag{4.4}$$

where the equivalent control is defined as

$$u_{eq} = \frac{1}{g(\boldsymbol{\xi})}\left[-\hat{f}(\boldsymbol{\xi}) - a_2 e_3 - a_1 e_2 + \dddot{r}\right] \tag{4.5}$$

where $\hat{f}(\boldsymbol{\xi})$ is the an approximation of the dynamics described by $f(\boldsymbol{\xi})$ and the following inequality holds

$$\left|f(\boldsymbol{\xi}) - \hat{f}(\boldsymbol{\xi})\right| \leq C_F \tag{4.6}$$

This yields

$$\begin{aligned} \dot{V} &= s[f(\boldsymbol{\xi}) + a_2 e_3 + a_1 e_2 - \dddot{r} + u_{eq} - g(\boldsymbol{\xi})k \cdot sign(s)] \\ &= s[f(\boldsymbol{\xi}) - \hat{f}(\boldsymbol{\xi})] - g(\boldsymbol{\xi})k|s| \\ &\leq -\left[g(\boldsymbol{\xi})k - C_F\right]|s| \end{aligned}$$

By choosing $k = \frac{C_F}{G_0} + k_0,\ k_0 > 0$ and $0 < G_0 \leq g(\boldsymbol{\xi}),\ \forall \xi$

$$\dot{V} \leq -G_0 k_0 |s| \tag{4.7}$$

By using the Comparison Lemma (Khalil, 2000, Chap. 3) it can be shown that

$$|s(t)| \leq |s(0)| - G_0 k_0 t,\ \forall\ |s(t)| > 0 \tag{4.8}$$

(Proof of (4.8) can be found in Appendix A.1) Therefore, trajectories starting outside the surface S will reach the surface in finite time, and once the surface is reached, the trajectory will stay on it for all future time, as seen from the inequality $\dot{V} \leq -G_0 k_0 |s|$.

The motion of the system now consists of a *reaching phase* when the trajectories starting outside of S converge to the surface in finite time, as seen from (4.8). Once the trajectory reaches the surface the system enters the *sliding phase*, and the motion of the system is now confined to the surface and the dynamics of the system is reduced to the second-order linear model $e_3 = -a_2e_2 - a_1e_1$.

Since $\dot{V}$ is only negative semidefinite, LaSalle's invariance principle must be applied to the system to formalise the stability analysis of the controller. Defining the set $H = \{x \in R^n \mid \dot{V} = 0\}$ which actually corresponds to the sliding surface S, and observing that based on (4.2) no solution can stay identically in S other than the trivial solution $e(t) \equiv 0$. Then based on Corollary 4.2 (Khalil, 2000, Chap 4) the origin of the system is global asymptotic stable.

4.2 Boundary Layer Control

As described in Section 2.4, chattering is a problem that is encountered during a practical implementation of an ideal SMC. In this section a boundary layer controller is designed as

$$u = u_{eq} - k \cdot sat(\frac{s}{\epsilon}) \tag{4.9}$$

where k and u_{eq} is the same as for the ideal controller in Section 4.1.2.

4.2.1 Equivalent control

The equivalent control is the continuous part of the control input u, and its goal is to cancel some known nonlinearities to allow a lower switching gain of the discontinuous component in the sliding mode controller. As defined in (4.5) the equivalent control is defined as

$$u_{eq} = \frac{1}{g(\boldsymbol{\xi})}\left[-\hat{f}(\boldsymbol{\xi}) - a_2e_3 - a_1e_2 + \dddot{r}\right]$$

where $\hat{f}(\boldsymbol{\xi})$ is an approximation of the function $f(\boldsymbol{\xi})$. The expression used for $\hat{f}(\boldsymbol{\xi})$ is

$$\begin{aligned}\hat{f}(\boldsymbol{\xi}) = &-\frac{1}{\hat{M}}\left[\frac{A}{(\hat{V}_0 + \hat{A}\xi_1)}\xi_2\left(\hat{M}\xi_3 + \hat{K}_l(1 - e^{-\hat{L}_l\xi_1}) - \hat{M}_l\xi_1 + \hat{D}\xi_2 + \hat{A}\hat{P}_0\right)\right] \\ &+ \frac{1}{\hat{M}}\left[-\hat{K}_l\hat{L}_l\xi_2e^{-\hat{L}_l\xi_1} + \hat{M}_l\xi_2 - \hat{D}\xi_3\right]\end{aligned} \tag{4.10}$$

where $\hat{K}_l, \hat{L}_l, \hat{M}_l, , \hat{V}_0$, $\hat{P}_0$ $\hat{D}$ and $\hat{M}$ are approximated values the respective parameters.

4.2.2 STABILITY ANALYSIS

Considering the Lyapunov-like function $V = \frac{1}{2}s^2$ the time-derivative satisfies the inequality

$$\dot{V} \leq -G_0 k_0 |s|$$

when $|s| \geq \epsilon$, i.e. outside the boundary layer. Therefore, as shown in (4.8) if $|s(0)| > \epsilon$, $|s(t)|$ will reach the set $|s| \leq \epsilon$ in finite time and remain in it for all future time. Inside the boundary layer the behavior of the system is shown in A.2. Therefore all trajectories will approach the set

$$\Omega_\epsilon = \left\{ |e_1| \leq \frac{\epsilon}{a_1}, |e_2| \leq \frac{\epsilon a_2}{a_2^2 - a_1}, |s| \leq \epsilon \right\} \tag{4.11}$$

Given $a_2 > \sqrt{a_1} > 0$. This means that the controller in (4.9) does not stabilize the origin of the system but it achieves ultimate boundedness, with an ultimate bound that is proportional to ϵ.

The stability analysis inside Ω_ϵ is done by studying a linearized model around the equilibrium point of the system, and is only performed for a constant reference i.e. $r = c$. The details of these calculations can be found in A.3, and the stability properties near the equilibrium point $\bar{\mathbf{e}} = [0 \ 0 \ 0]^T$ can be found by finding the eigenvalues of A_δ (The expression for A_δ is given in Appendix A.3.2). Figure 4.1 shows how the three eigenvalues of A_δ moves when the reference value moves from 1mm to 20mm which is the region of the reference used in the clutch sequence. As the plots show the real parts of the eigenvalues stay in the left half plane rendering the equilibrium point of the linearized system stable. Since two of the eigenvalues are complex conjugate the equilibrium point is in fact a stable focus. As described by Khalil (2000) it is reasonable to expect that the trajectories of the nonlinear system in a small neighborhood of the equilibrium point will be close to the trajectories of the linearized system. Therefore the equilibrium point $\bar{\mathbf{e}}$ of the nonlinear system will behave like a stable focus.

4.3 ADDITIONAL CONTROL ELEMENTS

4.3.1 INVERSE FLOW MODEL

In the model in (3.9) the input to the system is defined to be the mass flow rate (ω) in and out of the actuator. Therefore the output from the controller designed in this chapter is defined as desired flow. The inputs to both the simulation model and the real physical system are control signals to the supply and exhaust valves, and therefore an inverse

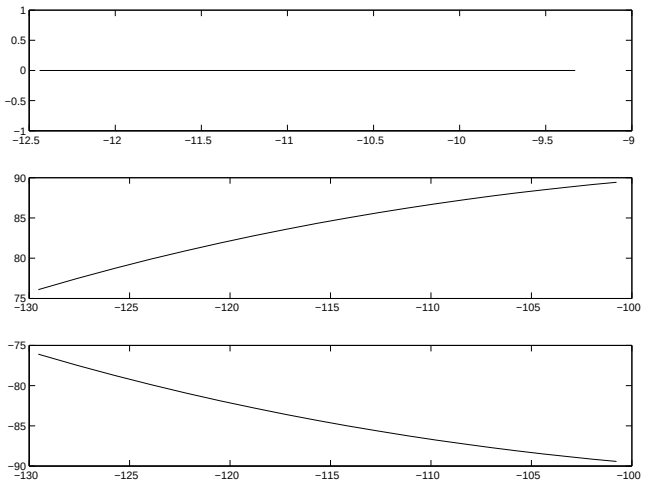

Figure 4.1: Eigenvalues of A_δ in the complex plane, showing that all three eigenvalues have a negative real part

flow model is required to calculate the valve control signals that correspond to the desired flow.

Since the output from the controller is the desired mass flow rate, the first task of the inverse flow model is to allocate the flow to the supply and exhaust valves. This is done simply by the following equations

$$q_{vs} = sat_{[0,\inf\rangle}\left(\omega_d\right) \tag{4.12}$$

$$q_{ve} = sat_{[0,\inf\rangle}\left(-\omega_d\right) \tag{4.13}$$

which only means that the positive part of the flow is allocated to the supply valve and the negative part to the exhaust valve. The next task is to find the desired valve opening based on the desired flow through each of the valves. This is done based on the flow model

$$q_v(p_h, p_l, C, B, u_v, \Theta_v) = g_v(p_h, p_l, C, B) \cdot y_v(u_v, \Theta_v) \tag{4.14}$$

where q_v represents the flow through one valve, g_v describes the flow capacity and y_v is the valve opening. The flow opening for a desired flow is now found through a regularized inverse

$$y_v = \frac{q_v}{max\left\{G_{lb}, g_v(p_h, p_l, C, B)\right\}} \tag{4.15}$$

where $G_{lb} > 0$ is a constant introduced to avoid division by zero (e.g. $G_{lb} = 10^{-4}$). The last part of the inverse flow model is concerned with finding the valve input

corresponding to the desired valve opening, y_v. This is done using the inverse PWM characteristic, $h_v^{-1}(y_v, \Theta_v)$. In practice the PWM characteristic $h_v(y_v, \Theta_v)$ is described by a lookup table. The valve input signal is then found by

$$u_v = \begin{cases} h_v^{-1}(y_v, \Theta_v) \ , \ y_v > Y_{lb} \\ 0 \ , \ y_v < Y_{lb} \end{cases} \tag{4.16}$$

where $Y_{lb} > 0$ is a small constant introducing a dead band around $y_v = 0$. More details concerning the inverse flow model can be found in (Kaasa, 2003).

4.3.2 RELAX VALVES

Relax valves is a logic block that is designed to calm down the control signals when the position approaches zero. Described in plain text the functionality of the relax valves block is that when the position, y and the desired position, y_d are below predefined thresholds and the desired velocity, v_d is zero or negative the supply valve is closed and the exhaust valve is fully opened for T_open seconds and then both valves remain closed while the conditions above still holds. When the conditions are not true the output is simply equal to the input.

Figure 4.2 clearly shows the effects that relax valves has on the control signal, especially to the exhaust valve when the position approaches zero. The reason that the signal is very noisy without this logic is that the flow capacity is very small, since the pressure is low and therefore small variations in the desired flow causes large values on the valve input.

4.3.3 REFERENCE TRAJECTORY FILTER

The controller designed in this thesis needs the desired trajectory and its first 3 derivatives to be continuous and smooth, and given the clutch sequence in Figure 6.1 a reference trajectory filter is needed. Introducing $z = [y_r \ \dot{y}_r \ \ddot{y}_r \ \dddot{y}_r]^T$ and defining the linear system

$$\dot{z} = \begin{bmatrix} 0 & 1 & 0 & 0 \\ 0 & 0 & 1 & 0 \\ 0 & 0 & 0 & 1 \\ -k_0 & -k_1 & -k_2 & -k_3 \end{bmatrix} z + \begin{bmatrix} 0 \\ 0 \\ 0 \\ k_0 \end{bmatrix} r$$

The characteristic polynomial of this system is

$$q = s^4 + k_3 s^3 + k_2 s^2 + k_1 s + k_0$$

The choice of the filter constants $k_i, \ i = 0, .., 3$ will decide the eigenvalues of the filter. If all the eigenvalues are to be placed at $\lambda_i = -\lambda_w, \ i = 0, .., 3$ the characteristic

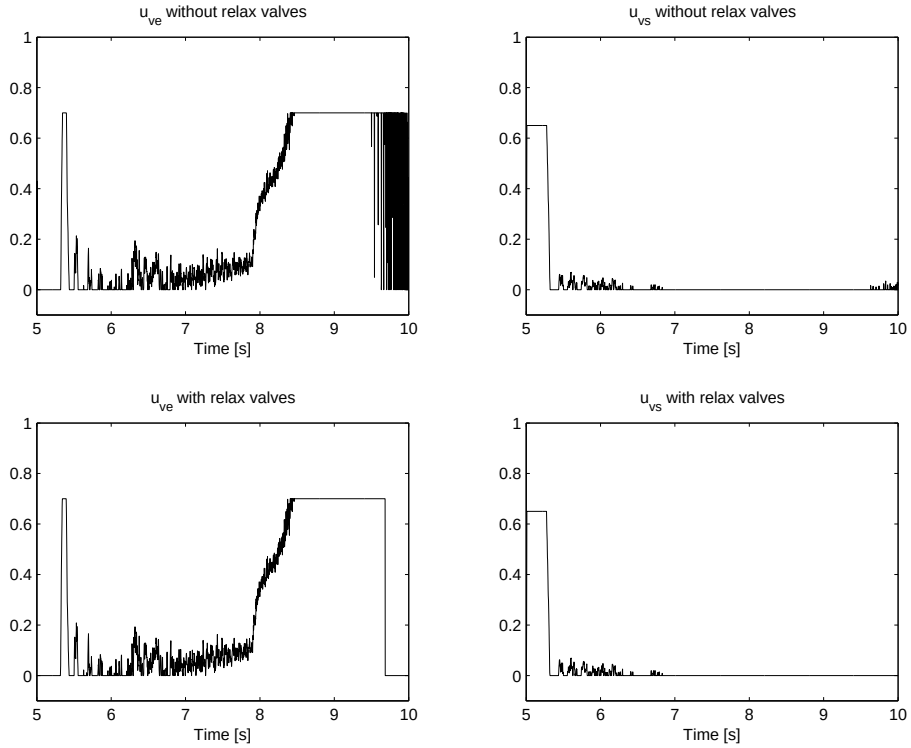

Figure 4.2: Plot of valve inputs with and without relax valves

polynomial of the filter should be

$$(s + \lambda_w)^4 = s^4 + 4\lambda_w s^3 + 6\lambda_w^2 s^2 4\lambda_w^3 s + \lambda_w^4$$

which yields the following values for the filter coefficients

$$\begin{aligned} k_0 &= \lambda_w^4 \\ k_1 &= 4\lambda_w^3 \\ k_2 &= 6\lambda_w^2 \\ k_3 &= 4\lambda_w \end{aligned}$$

making the filter Hurwitz with all eigenvalues placed at λ_w and a time constant $T = \frac{5}{\lambda_w}$. As Lokken (2006) describes, experimental results show that a 10 millisecond time constant is appropriate for use in heavy duty trucks. The corresponding eigenvalues of the filter is then $\lambda_w = 50$.

4.3.4 VELOCITY AND ACCELERATION

The position is the only measured variable in the system and since the controller requires both velocity and acceleration, estimates must be calculated. For this purpose a filter much like the reference trajectory filter was designed to estimate velocity and acceleration. Introducing the state estimate vector $\hat{x} = [\hat{x}_1 \ \hat{x}_2]$, and defining the linear system

$$\dot{\hat{x}} = \begin{bmatrix} 0 & 1 \\ -k_0 & -k_1 \end{bmatrix} \hat{x} + \begin{bmatrix} 0 \\ k_0 \end{bmatrix} x_{1,m}$$

where $x_{1,m}$ is the measurement of the variable x_1. The characteristic polynomial is for this system

$$q = s^2 + k_1 s + k_0$$

To place both the eigenvalues of the system at $\lambda_i = -\lambda$ the filter coefficients are chosen from

$$(s + \lambda)^2 = s^2 + 2\lambda s + \lambda^2$$

This gives $k_1 = 2\lambda$ and $k_0 = \lambda^2$. The value of $\hat{x}_2$ is now a filtered estimate of the derivative of the measurement $x_{1,m}$.

The velocity and acceleration estimator is then constructed from a cascade of two of these filters.

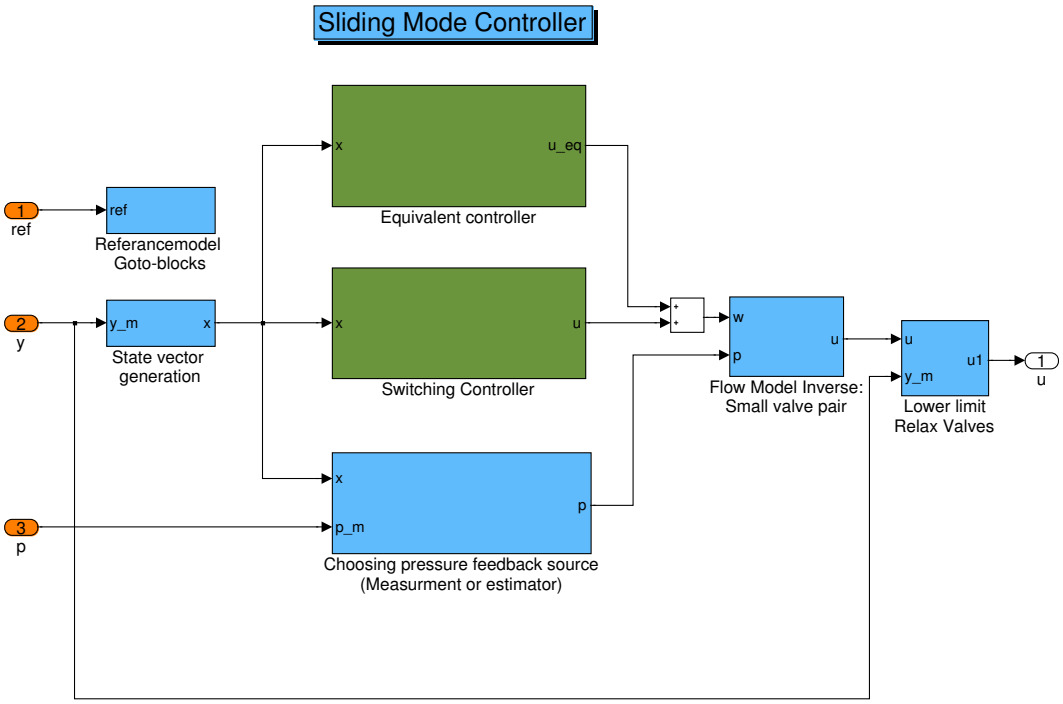

Figure 4.3: Block diagram showing the structure of the complete control system

The block diagram in 4.3 shows the structure of the complete control system when all the components described in this chapter is implemented.

CHAPTER 5

CONTROLLER EXTENSIONS

In this chapter some extensions of the controller designed in Chapter 4 are introduced, and their effect on the controller performance is evaluated.

5.1 PRESSURE ESTIMATOR

In the present configuration the clutch actuation system has two measurements, position and pressure. As usual in the automotive industry it is desirable to remove non-essential components to reduce the total cost of each unit, and since the pressure measurement is only used in the inverse flow model a very accurate estimate of the pressure is not required. Since the physical laws governing the pressure in the cylinder is rather well known a pressure estimator can be designed to allow the removal of the pressure sensor. The estimator is simply based on the following relation found from (3.4)

$$M\dot{v} = -f_l(y) - f_f(v, y_f) + A[p - P_0]$$

giving the following expression for the pressure in the cylinder

$$\hat{p} = \frac{1}{A}\left[M\dot{v} + f_l(y) + f_f(v, y_f)\right] + P_0 \tag{5.1}$$

$f_l(y)$ is calculated using the load characteristic model based on gaussian basis function and is therefore rather accurate. For the friction force, $f_f(v, y_f)$ both viscous and LuGre friction models were tested. Figure 5.1 shows a plot of the measured and estimated pressure during a typical clutch sequence when viscous friction is used in the pressure estimator. The same plot when the LuGre-friction model was used in the pressure estimator is presented in Figure 5.2.

Simulations of the system using both the friction models show almost identical performance of the controller when estimated pressure is used compared to measured pressure. Even when the sample time is increased to 10ms the differences in performance are practically non-existent. Though the pressure estimator has only been tested in computer simulations these give good indications that this will work very good also on a physical system and therefore the pressure measurement is probably obsolete.

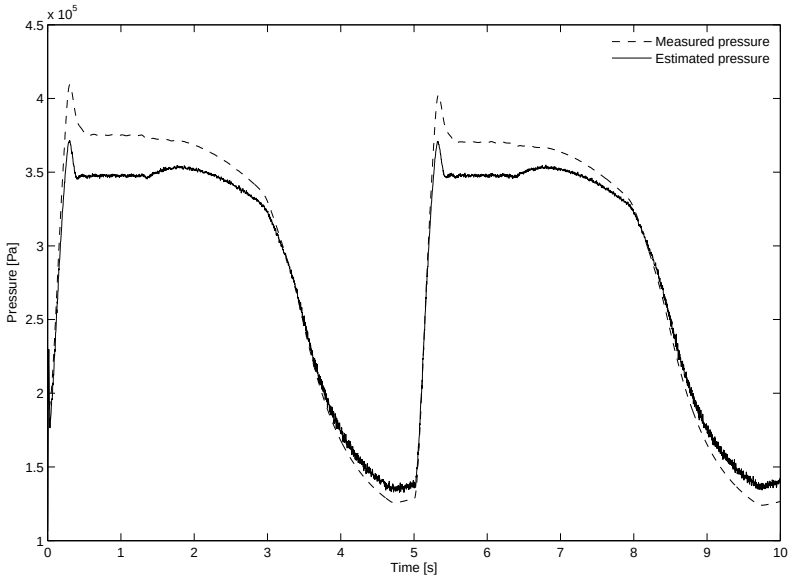

Figure 5.1: Measured and estimated pressure when using viscous friction

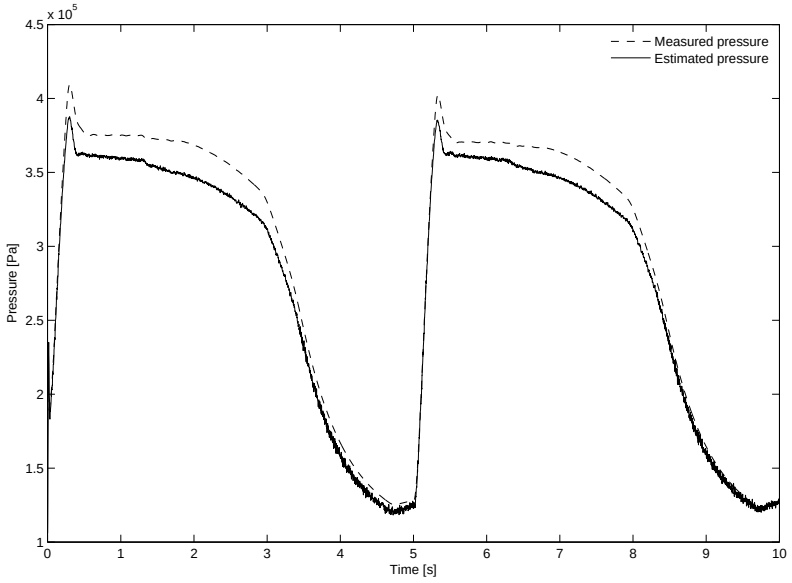

Figure 5.2: Measured and estimated pressure when using LuGre friction

5.2 LuGre-friction model

Since the viscous friction model used in the controller design in Chapter 4 is very simplified compared to the real friction in the system, an extension to the more accurate LuGre-friction model is considered. The model for the controller design would then be extended to a 4^{th}-order model, where the dynamics of the new state y_f is considered as the internal dynamics of the system, which means that the relative degree of the system remains unchanged. The new model would then be

$$\begin{aligned} \dot{y} &= v \\ M\dot{v} &= -f_l(y) - f_f(v, y_f) + A[p - P_0] \\ \dot{p} &= \frac{1}{V(y)}(-Avp + RT_0 q_v) \\ \dot{y}_f &= g_f(v, y_f) \end{aligned} \tag{5.2}$$

where the variables and expressions are the same as in Section 3.2. The only difference in the controller structure as a result of this new model will be a different equivalent control law and the introduction of a simple estimator for y_f. Figure 5.3 shows the calculated friction force and its time derivative with viscous and LuGre friction models used respectively. These plots show a significant difference between the two models. Results from computer simulations of the controller response with the two friction models can be found in Appendix B.1. These simulations actually show a deterioration in the performance of the controller when the more accurate LuGre-model is used. This can be seen as an indication of the sliding mode controller's robustness properties with respect to modelling errors, since better performance is not achieved with a more realistic model. Since friction often is one of the most difficult effects to model in a physical system it might be a big advantage to have a controller that does not rely heavily on the accuracy of the friction model.

5.3 Integral effect

As described by Khalil (2000) and Bouri and Thomasset (2001) the sliding mode controller can be augmented to include integral action by choosing the following sliding function

$$s(\mathbf{e}) = a_0 e_0 + a_1 e_1 + a_2 e_2 + e_3$$

where $e_0 \equiv \int e_1 dt$. The introduction of integral effect in the sliding mode controller will, as in a linear controller ensure zero steady-state error. The resulting motion on of the system in sliding mode (i.e. $s(\mathbf{e}) = 0$) will then be governed by

$$e_3 = -a_2 e_2 - a_1 e_1 - a_0 e_0 \tag{5.3}$$

given that $a_0, a_1, a_2 > 0$ this implies that $e_1(t)$ converges to zero as t tends to infinity. The stability analysis of this controller is rather similar to the controller without integral effect and the details of these analysis can be found in Appendix A.3.3.

The plots in Figure 5.4 show the effect of the integral action when applied to a constant reference compared to no integral action. The figure clearly shows that the introduction of integral effect in the controller achieves what it was designed for, namely to ensure zero steady-state error. Even though the integral action yields the desired performance, the figure also shows that the steady-state error without integral action is actually a lot smaller than the amplitude of the measurement noise and is of little importance. The reason that integral effect has still been introduced is that experimental testing with other controllers on the clutch-system has shown steady-state error when tracking a constant or nearly constant reference near the slip-point of the clutch (i.e. 7-11 mm). This error occurs because the clutch discs actually expand causing a steady-state error. Since this is an effect that does not occur in the simulation model, and tests with this kind of reference has not been tested on a physical test rig with the SMC it is uncertain whether this problem would occur also with this controller.

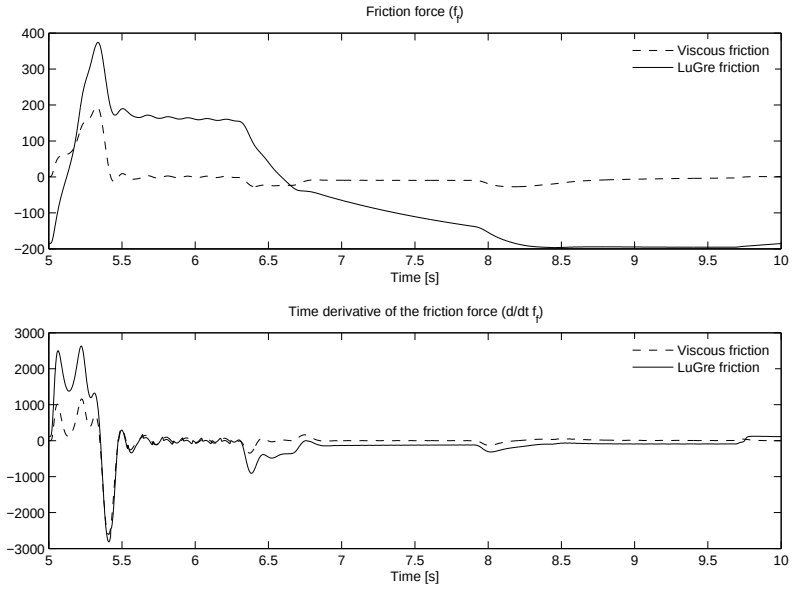

Figure 5.3: Calculated friction force (f_f) and its time derivative ($\frac{d}{dt}f_f$) with viscous friction model and LuGre-friction model during a typical clutch sequence

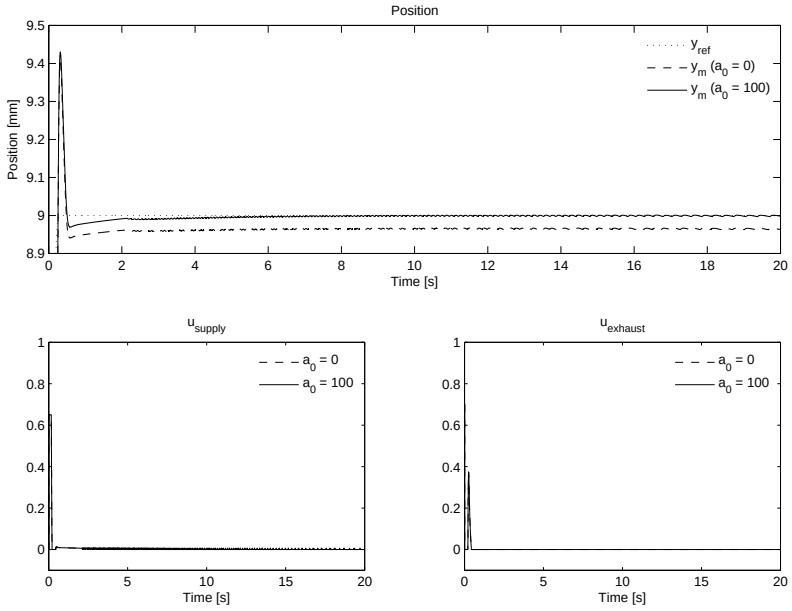

Figure 5.4: Simulation results from tests with constant reference and $a_0 = 0$ and $a_0 = 100$ respectively

CHAPTER 6

SIMULATION

In this chapter results from computer simulations of the controller designed in Section 4.2 are presented. The model used for to test the controller is described in Section 3.1. Both the simulation model and the controllers have been implemented using MatLab® and Simulink®.

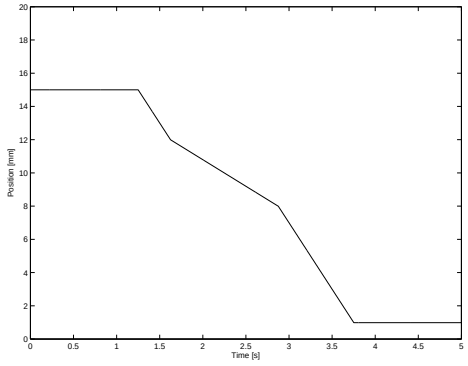

Figure 6.1: Plot of a typical clutch sequence

Figure 6.1 shows the clutch sequence that was used as a reference when testing the controller. The simulations were as mentioned earlier done in Simulink. They were conducted using an ODE-5 (Dormand-Price) fixed-step solver with 2ms integration step size.

Figure 6.2 contains bar graphs showing RMS and maximum errors in the different test cases. The RMS-value is defined as

$$e_{rms} = \sqrt{\frac{\sum_{i=1}^{N}(y_i - r_i)^2}{N}}$$

where y_i is the measurement at time step i, r_i is the desired position at time step i and N is the total number of available measurements.

The tuning of the controller constants were done by trial and error and the following

values were used in the simulations: k = 0.017, ϵ = 8, a_1 = 1050 and a_2 = 95. The eigenvalues of the velocity and acceleration filters designed in Section 4.3.4 are chosen by trial and error and in the simulations, $\lambda_v = 125$ and $\lambda_a = 70$ is chosen for the velocity and acceleration filters respectively.

6.1 TEST PLAN

The main concern of this thesis has been to design a robust controller for the clutch-actuation system. Therefore robustness has been the most important factor when designing a test plan for the computer simulations.

1. No noise, nominal values used in the controller
2. Noise added to the position measurement, nominal values used in the controller
3. Noise added to the position measurement, $f_l(y)$ is 1000N lower in the controller than the nominal value
4. Noise added to the position measurement, $f_l(y)$ is 1000N higher in the controller than the nominal value
5. Noise added to the position measurement, $f_l(y)$ is 1000N higher in the controller than the nominal value and the V_0 is increased by 50%
6. Noise added to the position measurement, $f_l(y)$ is 1000N higher in the controller than the nominal value and the V_0 is decreased by 50%

6.2 SIMULATION RESULTS

Figures 6.3 to Figure 6.8 show plots of position (y), input to supply valve (u_{vs}) and exhaust valve (u_{ve}).

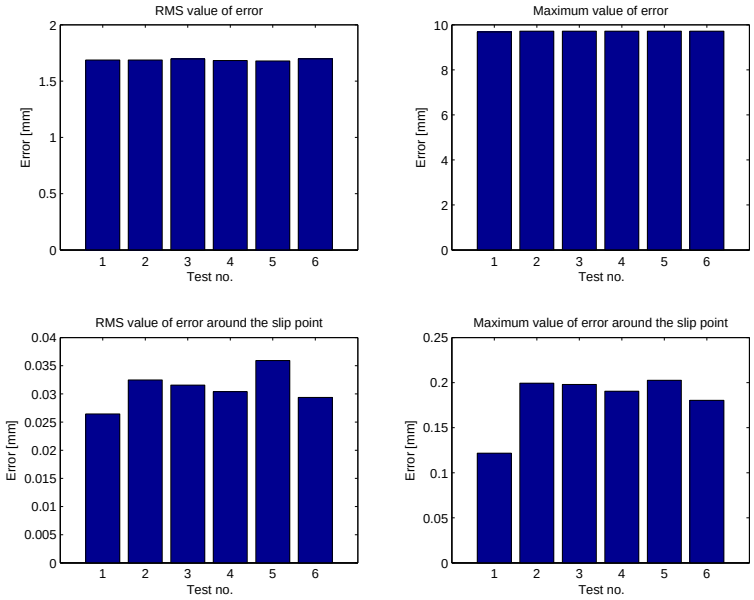

Figure 6.2: Comparison of maximum and RMS values of the tracking error in the different test cases

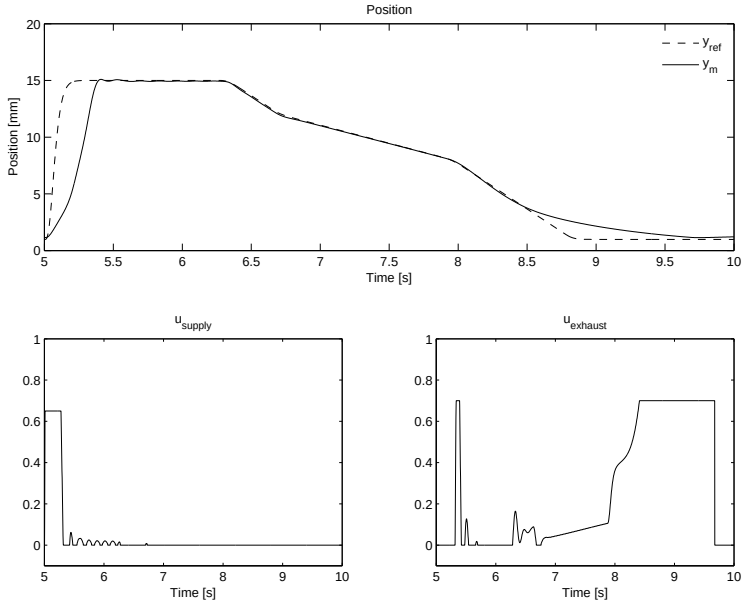

Figure 6.3: Case 1: No noise, nominal values on controller constants

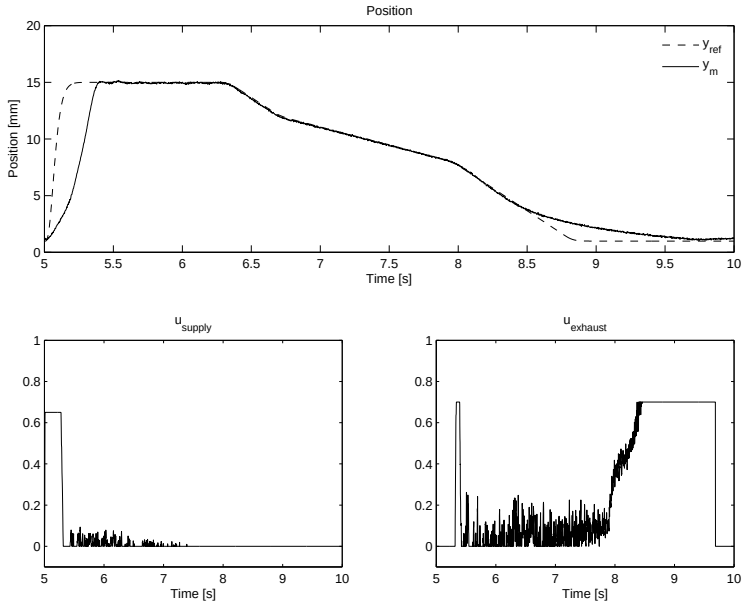

Figure 6.4: Case 2: White noise added to position measurement, nominal values on controller constants

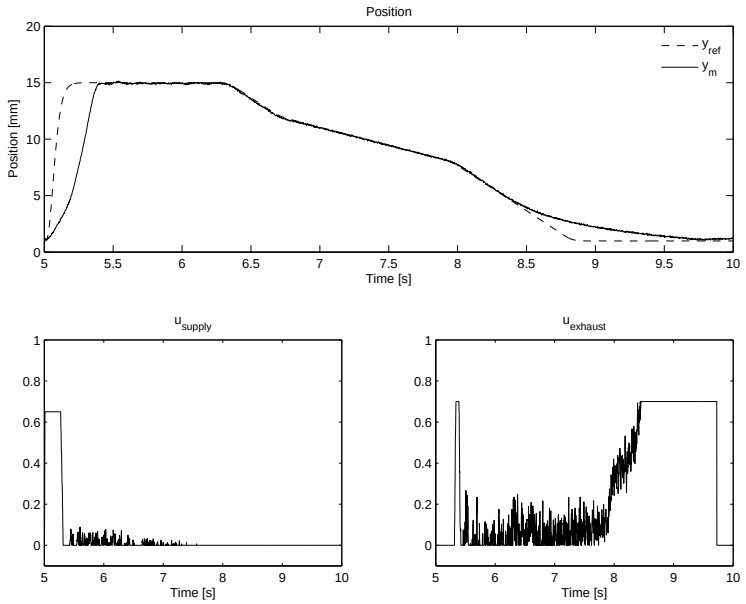

Figure 6.5: Case 3: Load characteristic lowered 1000N in the controller compared to the nominal values

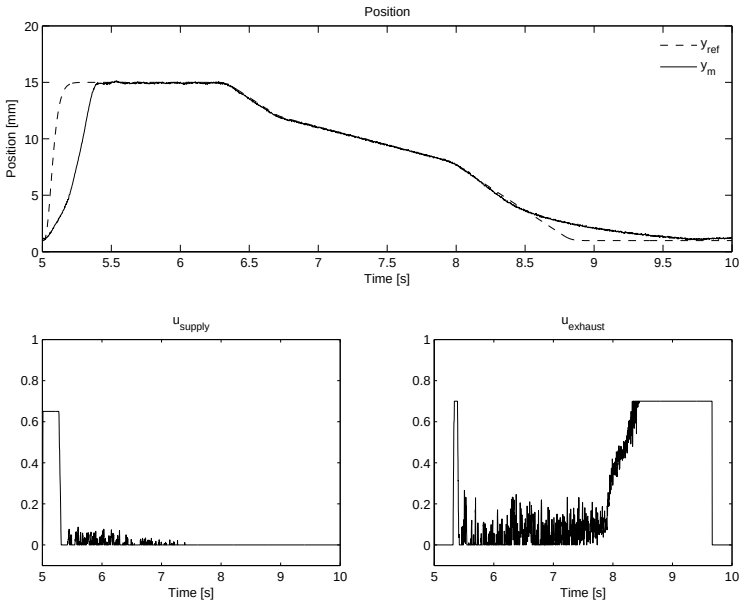

Figure 6.6: Case 4: Load characteristic higher 1000N in the controller compared to the nominal values

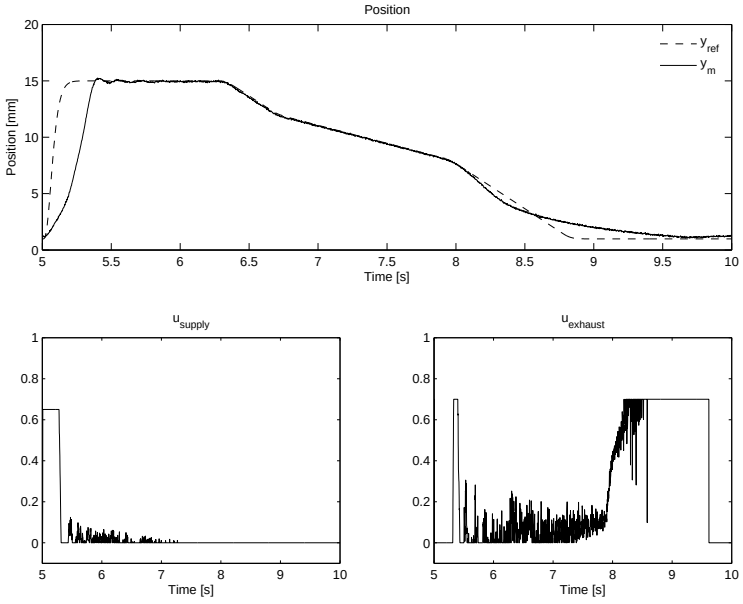

Figure 6.7: Case 5: Load characteristic raised 1000N in the controller compared to the nominal values AND initial volume increased by 50%

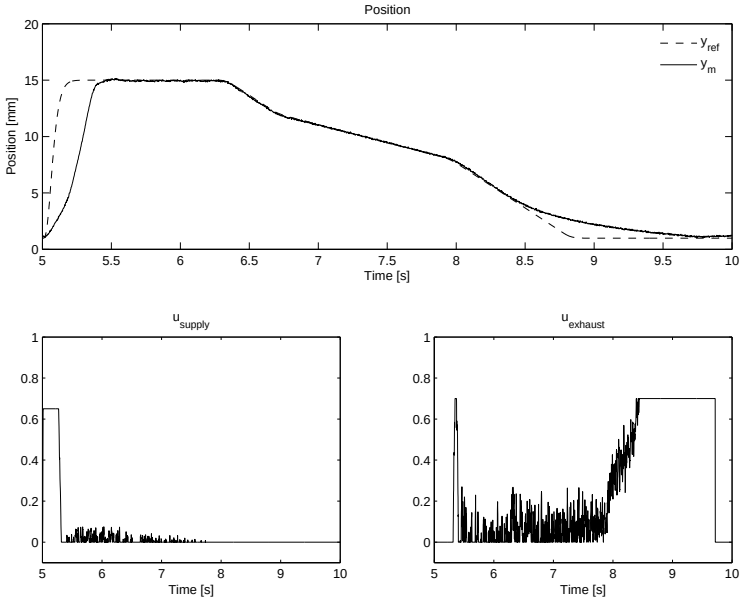

Figure 6.8: Case 6: Load characteristic raised 1000N in the controller compared to the nominal values AND initial volume decreased by 50%

6.3 COMMENTS

The simulation results shown in the previous section show a good tracking performance of the boundary layer controller. The lack of tracking precision in the start of the clutch sequence is caused by physical limitations of the flow into chamber A. Better performance in this region cannot be achieved with a different control strategy, but requires a larger supply valve. The lack of precision in the last part of the clutch sequence is also a system dependent problem, since the flow through the exhaust valve is dependent on the pressure in chamber A, and therefore when the pressure drops so does the potential flow out of chamber A.

The rather noisy input signals to the valves is not a big problem since PWM is used to control the valves. This only means that the duty cycle of the PWM signal changes between two consecutive PWM periods and this does not cause any more mechanical wear and tear.

The very distinct ramp on the input of the exhaust valve at the end of the clutch sequence occurs because of the *relax valves* part of the controller as described in Section 4.3.2.

CHAPTER 7

EXPERIMENTAL RESULTS

In this chapter results from experimental testing of the controllers from Chapter 4 are presented. The tests were carried out in the test lab at Kongsberg Automotive.

7.1 THE TEST RIG

Most of the tests were performed on a test rig at KA's test lab. The test rig was consists of a KA PCA (Pneumatic concentric actuator) with a pneumatic area of 0.0235 m^2, two 4mm On/Off valves and a Valeo push type clutch. The controller was implemented on a dSpace MABX DS1401 unit. Additionally a driver circuit, based on a modified H-bridge was used to achieve a faster discharge of the coil which open and close the valves.

7.2 ROBUSTNESS TESTS

Since the main focus of this thesis is to test the robustness of a Sliding Mode Controller for the electro-pneumatic clutch actuation system a series of tests were conducted to evaluate the performance of the controller with rather large parameter variations. The following test plan was derived for this purpose

1. Nominal values used in the controller
2. $f_l(y)$ is 1000N lower in the controller than the nominal value
3. $f_l(y)$ is 1000N higher in the controller than the nominal value
4. $f_l(y)$ is 1000N higher in the controller than the nominal value and the V_0 is increased by 50%
5. $f_l(y)$ is 1000N higher in the controller than the nominal value and the V_0 is decreased by 50%

7.2.1 TESTS WITH 2MS SAMPLE TIME

The results from the robustness tests with 2ms sample time are presented in Figures 7.2 to 7.6. Figure 7.1 contains bar graphs showing RMS and maximum errors in the different test cases.

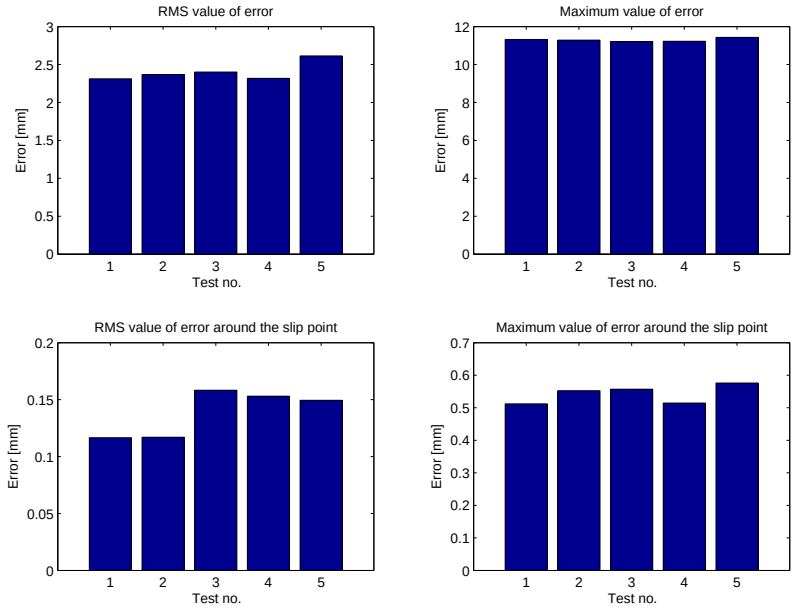

Figure 7.1: Comparison of maximum and RMS values of the tracking error in the different test cases

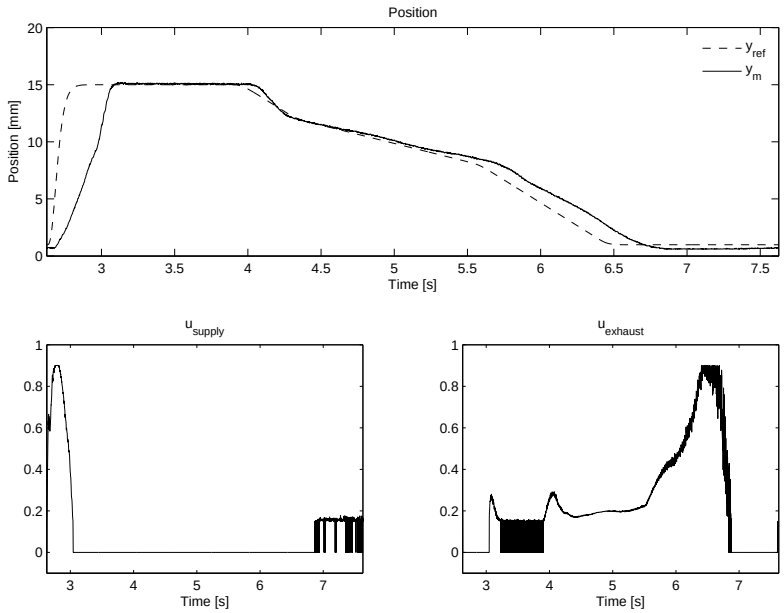

Figure 7.2: Case 1: Nominal values in the controller

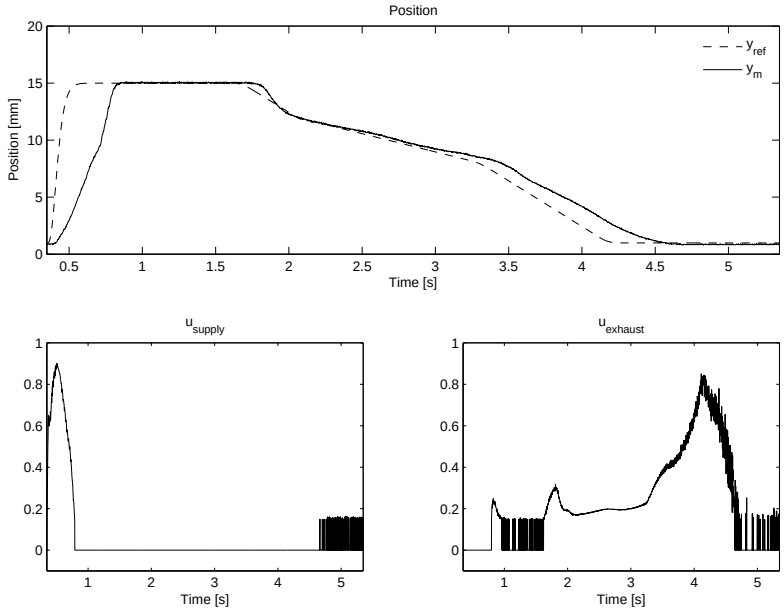

Figure 7.3: Case 2: Load characteristic lowered 1000N in the controller compared to the nominal values

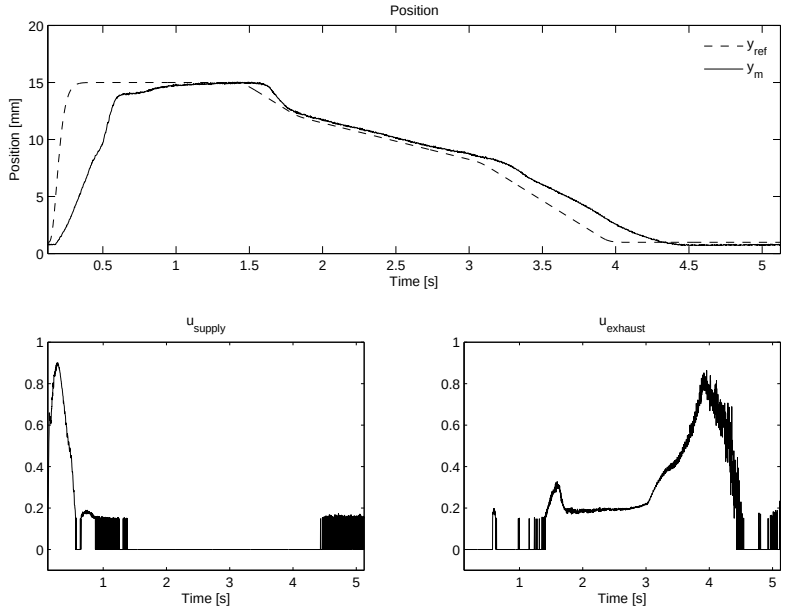

Figure 7.4: Case 3: Load characteristic raised 1000N in the controller compared to the nominal values

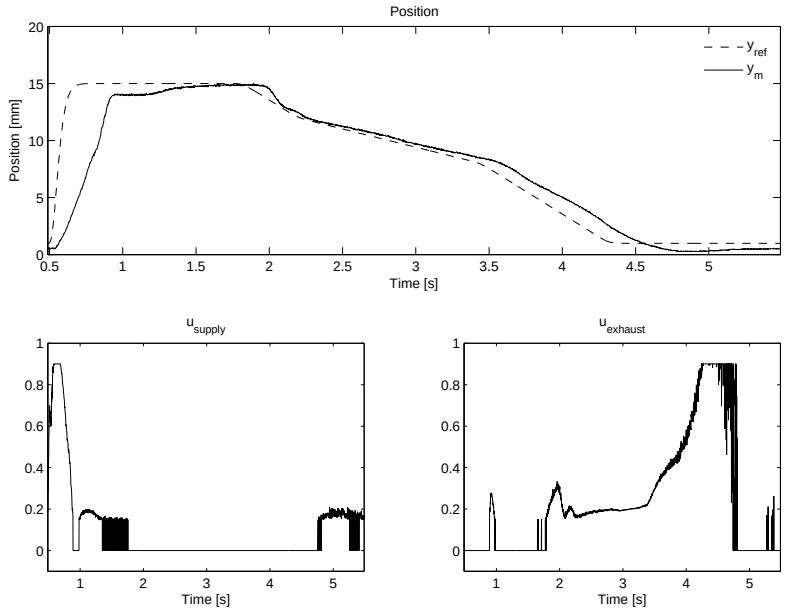

Figure 7.5: Case 4: Load characteristic raised 1000N in the controller compared to the nominal values AND initial volume increased by 50%

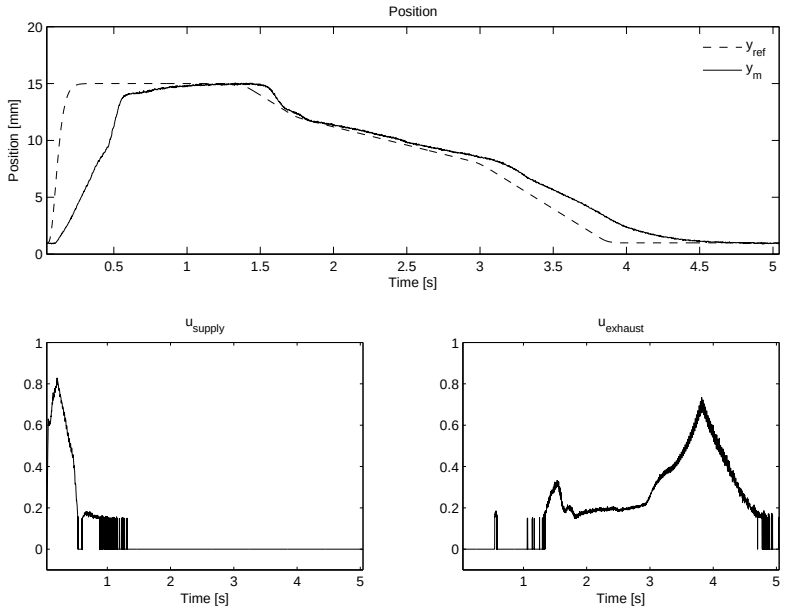

Figure 7.6: Case 5: Load characteristic raised 1000N in the controller compared to the nominal values AND initial volume decreased by 50%

7.2.2 TESTS WITH 10MS SAMPLE TIME

The controller was also tested with a 10ms sample time since this is the desired sample time in a commercial implementation in a truck. The graphs in Figure 7.7 show the RMS and maximum errors in the different test cases. The results are presented in Appendix B.2

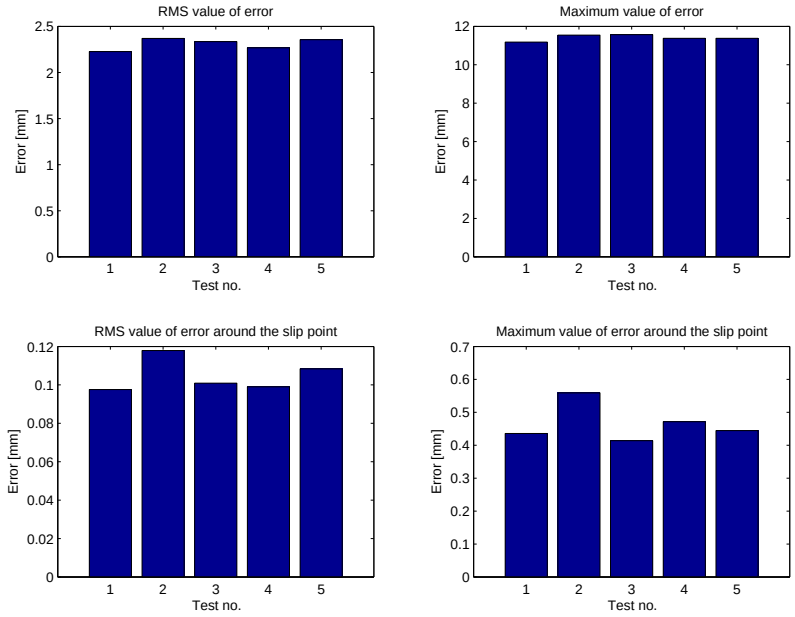

Figure 7.7: Comparison of maximum and RMS values of the tracking error in the different test cases

7.3 COMPARISON WITH PD AND BACKSTEPPING

Since both a PD-controller and several Backstepping controllers have already been designed and implemented for the clutch actuation system, a comparison between them and the Sliding Mode Controller was also important. In this section results from comparison tests performed at the test rig are presented.

7.3.1 CLUTCH SEQUENCE

First the three controllers were tested with a typical clutch sequence. The results are presented in Figures 7.8 to 7.10

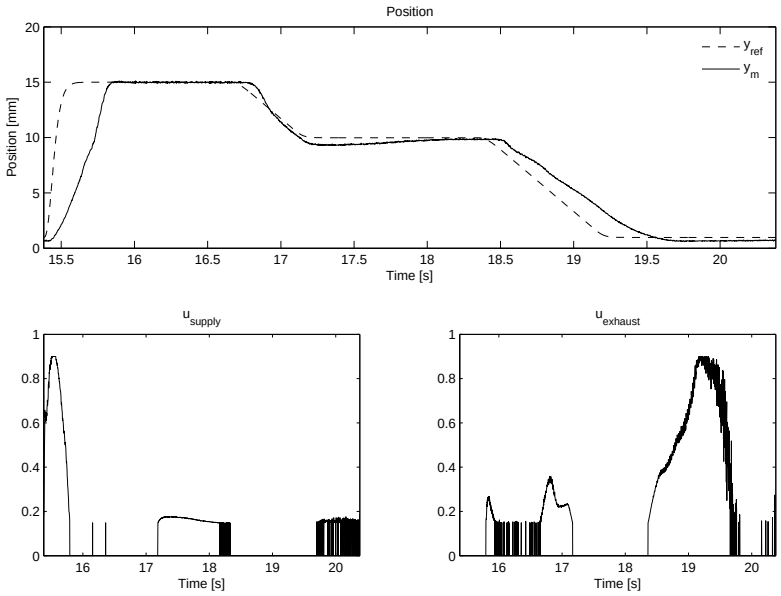

Figure 7.8: Clutch sequence tested with Sliding Mode Controller

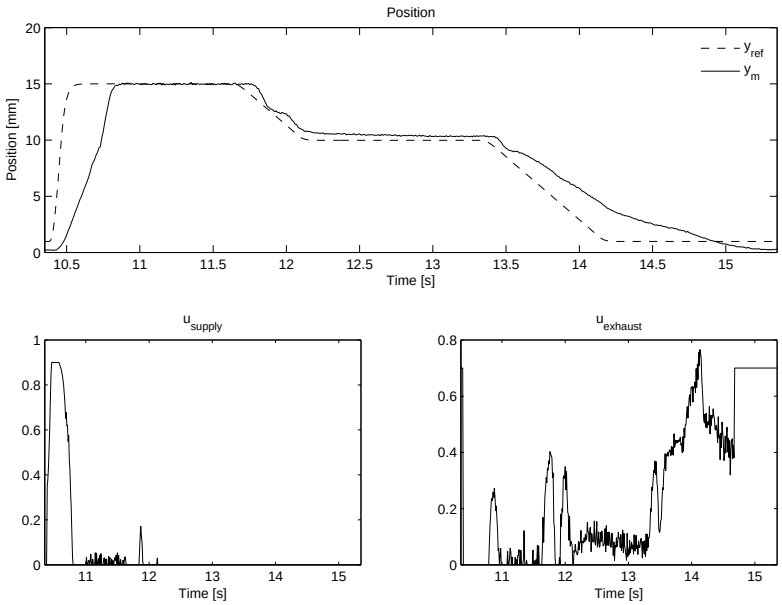

Figure 7.9: Clutch sequence tested with PD controller

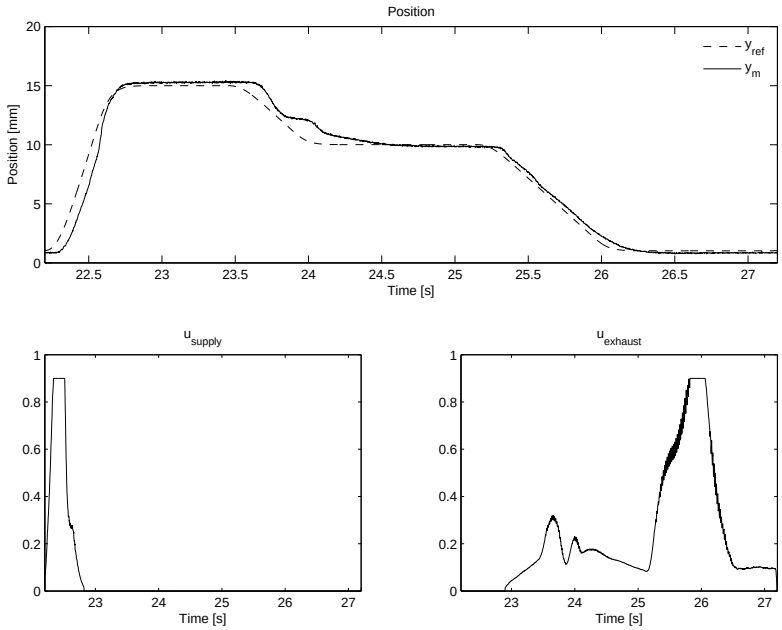

Figure 7.10: Clutch sequence tested with Backstepping controller

7.3.2 RANDOM REFERENCE

The controllers were also tested with a random reference to check the performance with a more general reference e.g. from a clutch pedal in a CBW system. The results are presented in Appendix B.3.

7.4 CAR TESTING

To test the controller in an even more realistic enviroment, some tests were performed in a Scania Truck at KA. The performance of the sliding mode controller and a PD controller for comparison are presented in Figures 7.11 and 7.12

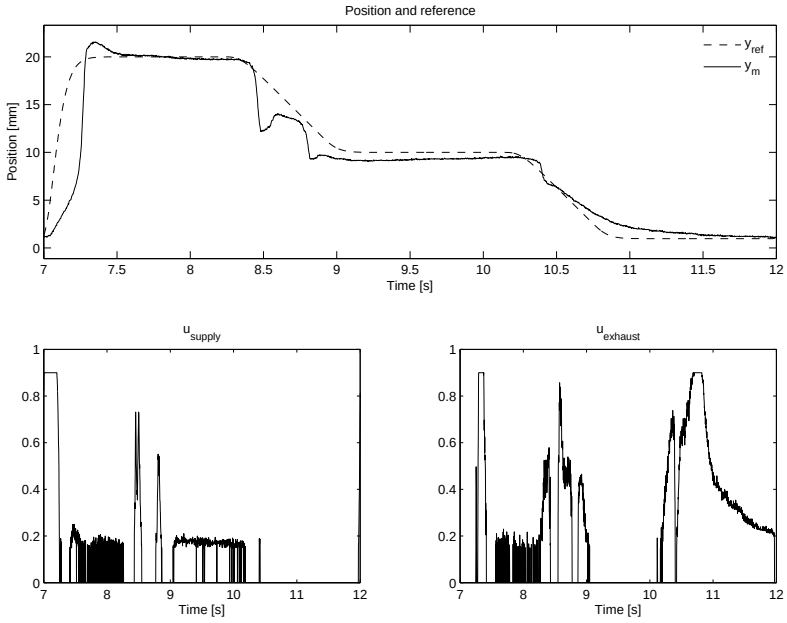

Figure 7.11: Results from car testing of the Sliding mode controller

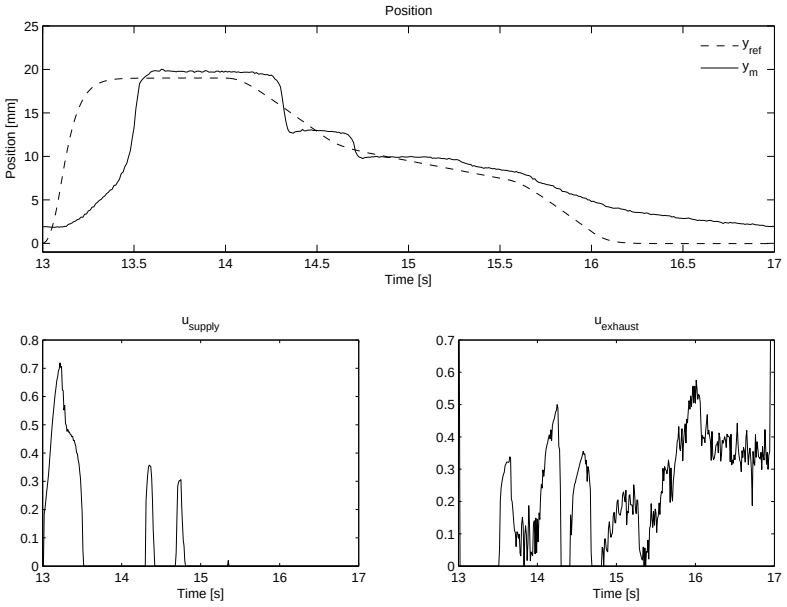

Figure 7.12: Results from car testing of the PD controller

7.5.1 RIG TESTING: ROBUSTNESS TESTS

The results presented in Section 7.2 show a rather good tracking performance of the SMC in experimental tests. Compared to the simulation results in Section 6.2 there are some differences in the performance of the controller, but also many similarities. The differences may be caused by several things, but the most significant factor is that the simulation model used for verification is based on a system with another load characteristic and different valves than in the rig at KA. Other factors may include unmodelled dynamics, external disturbances etc.

Despite these differences the experimental results also show many of the same features as the simulation results indicated, including the robustness properties with respect to parameter uncertainty and modelling errors. As the graphs in Figure 7.1 show, the RMS and maximum errors are only slightly affected by rather significatnt parameter changes. As Figure 7.2 shows, an acceptable tracking performance is also achieved in the rig testing with the Sliding mode controller.

The controller was also tested with 10ms sample time since this is the sample time used in most automotive computers. As the results in Appendix B.2 show, rather good tracking performance is also achieved with this sample time. This could almost be expected since the duty cycle period of the PWM signal is 20ms, which means that a change in the output at a higher frequency than 50Hz will not be of any significance. The fact that there still are differences between 2ms and 10ms sample time is propably caused by a difference in the velocity and acceleration estimates. Though the tracking performance is rather good at 10ms smaple time, an unacceptable overshoot appears in some of the test cases. This is propably caused by less accurate velocity and acceleration estimates, and could possibly be avoided by a different tuning of the controller

7.5.2 RIG TESTING: COMPARISON TESTS

As mentioned in Section 7.3 tests were performed in the test rig to compare the performance of the sliding mode controller to the performance of both a PD and a Backstepping controller. The figures in Section 7.3.1 show the performance of the three controllers during a typical clutch sequence. An important fact to mention about these tests is that the backstepping controller was tested with a ”slower” referance trajectory filter ($\lambda_w = 50$ for the SMC and PD, $\lambda_w = 30$ for the Backstepping controller) than the other two controllers. This is done because the backstepping controller yields a poor

performance with a faster reference. The reason for this limitation in the Backstepping controller is that the derivatives of the reference are weighted heavily in the feedback, and a ”faster” trajectory filter will give larger reference derivatives which compromise the smoothness of the Backstepping controller. Though this might not be a very severe limitation of this controller, it is still an important difference from the SMC and PD controller and must be adressed in comparison between them.

The comparison with the Backstepping and PD controllers also reveals many similarities, but also some severe differences in the tracking performance. The biggest difference between the performance of three controllers is when the position approaches the slip point, that is between 1,5 and 2,5 seconds after the start of the clutch sequence. Here the SMC yields a smoother trajectory for the position, but it also gets negative overshoot when compared to the reference trajectory, while the Backstepping and PD controllers does not give the same smoothness in this region. The Backstepping controller is the fastest in reaching the reference in the slip-point area, while the PD-controller actually suffers from a steady-state error.

The control signals produced by the three controllers are also an issue that must be considered when comparing different control strategies. As mentioned earlier a noisy control signal is not a severe problem when PWM is used, except when the signal oscillates around zero duty cycle of the PWM. For instance if both the supply and exhaust valve is commanded to open for 30 % of the duty cycle period this would give the same result as to keep them both closed, and such oscillations leads to increased wear and tear of the valves. At this point the Backstepping controller is superior to the other two control straregies, as it produces a very smooth output. The SMC yields the most noisy control signal, which is not very surprising since control chattering is the biggest problem in practical SMCs.

The three controllers were also tested with a random reference generated from a joystick to emulate a reference trajectory that could be generated in a Clutch-by-wire application. This is done because a problem when tuning and testing controllers is that only one kind of reference is used and then the controller is tuned to follow this reference perfectly, but when applied to a different reference trajectory the controller may perform poorly. Results from these test are shown in Appendix B.3, and though the reference trajectories used for the different controllers are not similar they can give an indication of the performance differences. These results clearly show that the SMC’s performance is at least as good, if not better than that of the Backstepping controller. The biggest advantages of the SMC compared to the Backstepping controller are first a faster response, i.e. it tends to handle faster variations in the reference trajectory. Secondly the Backstepping controller gives bigger steady state error than with the SMC.

7.5.3 CAR TESTING

As mentioned in Section 7.4 tests were performed in a Scania Truck at KA. An important remark concerning these tests is that the clutch in this car is close to the stability limit and is therefore inherently difficult to control. The results in Figure 7.11 and 7.12 show a rather poor tracking performance of both the PD- and the SM-controller. The ”negative overshoot” experienced when engaging the clutch again after disengagement (i.e. 1.3-2 seconds into the clutch sequence) is typical for clutches with a load characteristic on the border of instability, and is experienced in most controllers applied to this system. Despite the poor performance of both controllers, the SMC yields a much better tracking than the PD-controller.

CHAPTER 8

CONCLUDING REMARKS

In this chapter, discussions of the results achieved throughout this thesis are presented. Also some concluding remarks regarding the contributions of this thesis to the problem of position tracking control of the electro-pneumatic clutch actuation system produced by Kongsberg Automotive ASA. Finally some recommendations for future work on the subject of Sliding mode control for this system are presented.

8.1 DISCUSSIONS

The results from computer simulations and experimental results presented in Chapter 6 and 7 show good tracking performance and robustness properties of the Sliding Mode Controller, yet there are some issues that must be addressed.

As the plots of the control signals generated by the SMC show these are quite noisy. Based on the theory in Section 2.4 this is not a surprising result, since control chattering is the biggest problem with practical sliding mode controllers. Though the results in Section 6.2 show the noise on the control signals disappears when the measurement is free of noise, indicating that the reason for this chattering is not mainly caused by the switching term in the controller. The use of the *boundary layer technique* for chattering avoidance actually reduces the control law to a linear PDD-controller with feedback linearisation inside the boundary layer, and thus the robustness wrt. measurement noise is compromised. Combined with the use of filtered derivatives for estimating the velocity and acceleration, the boundary layer controller produces rather noisy control signals. To avoid this effect, either less noisy estimates of the velocity and position must be found or a different chattering avoidance technique must be applied.

Even though the control signals are very noisy it is not as big a problem as it might seem, because of the use of PWM control. First as discussed in Section 7.5.2 when combining PWM with on/off-valves noise on the control signal does not necessarily lead to any more wear and tear of mechanical components. Secondly the sampling time of the controller is 2ms while the period time of the PWM is 20ms, meaning that only 10% of the values of the controller output actually leads to a change in the valve opening.

Since PD and Backstepping controllers have already been developed for the clutch actuation system, comparisons with these is also an important issue when evaluating the

sliding mode controller. Considering position tracking performance both the Backstepping controller and the SMC yields rather good results, though when evaluating the use of control action the Backstepping controller is superior to the SMC. These results alone would indicate the Backstepping controller as the best choice, but there are also other factors which must be discussed when comparing control strategies:

Robustness: Since the main focus of this thesis has been robustness of the controller, this is an important factor when comparing the SMC to other control strategies. The robustness properties of the sliding mode controller have been discussed earlier, and have been shown to be very good. On the other hand the performance of the Backstepping controller depends heavily on correct values of the model parameters, in particular a correct load characteristic is crucial.

Observer: The backstepping controller depends on a full state feedback and therefore a state observer has been designed. In the SMC only the velocity and acceleration is needed, and these could be found through derivation and low-pass filtering. The introduction of an observer might not seem like a problem, but it yields poor performance when the sample time is increased to 10ms as is desirable in commercial implementation. This again compromises the performance of the backstepping controller.

Size of the control law: A typical ”problem” for backstepping controllers is the size of the control law. This is a problem theoretically since it might be difficult to understand for others than the designer and it might complicated the tuning since it is not always intuitive to understand the effect the controller parameters. The size of the control law also causes difficulties in a practical implementation, especially in an automotive system since it is desirable to have as cheap components as possible. Combined with an observer the backstepping controller yields a computer implementation that requires a lot more space than an SMC, requiring the use of a computer with more memory and more calculation capability.

8.2 Conclusion

As stated in the problem formulation in Section 1.3, robustness is very important in the clutch actuation system considered in this thesis. The results presented show that the sliding mode controller have very good robustness properties with respect to parameter variations and modelling errors. Combining the robustness with satisfying tracking precision the controller achieves the goals of the problem formulation.

Comparisons with the backstepping controller reveals different strengths and weaknesses of the controllers, and these are discussed in Section 8.1. This thesis does not attempt to decide which is the best choice of controller for the electro-pneumatic clutch actuator, but concentrates on presenting the sliding mode controller as an alternative control strategy. Through tests it is shown that a controller based on this technique is a feasible choice. In addition, the results from Section 5.1 also eliminates the need for a pressure measurment in the control system. As mentioned earlier, cost of the components is often the most important issue in the automotive industry and the removal of the pressure measurment will contribute to a lower cost per unit.

8.3 Recommendations for future work

In Section 8.1 it is argued that the most severe problem of the sliding mode controller is the noisy control signals. One possible improvement of the controller presented in this thesis si the use of a different strategy of estimating the velocity and acceleration for instance by using a robust sliding mode differentiator as described by Levant (1998). Application of a different chattering handling technique might also be worth investigating. As presented in the litterature review different methods for chattering avoidance have been developed, though many of them are still in an early phase of research and might not be ready for a practical implementation yet. Still this is an important issue, and alternatives to the boundary layer technique should be investigated.

The model used for the control design is very simplified compared to the simulation model, and even though the results from tests with the LuGre-friction model instead of only viscous friction indicates that more accurate models does not improve the performance of the controller, it is worth looking into using a more complex model.

More experimental testing should also be performed both additional robustness tests and a more extensive comparison with the backstepping to get an better understanding of the differences in performance of the two controllers.

BIBLIOGRAPHY

Bouri, M. and Thomasset, D., 2001. "Sliding control of an electropneumatic actuator using an integral switching surface", *IEEE Transactions on control systems technology*, Vol. **9**, no. 2.

Bouri, M., Thomasset, D., E.Richard, and S.Scavarda, 1994. "Nonlinear sliding mode control of an electropneumatic servodrive", *7th Bath Int. Fluid Power Workshop, Innovations in Fluid Power,*, Vol. , pp. 201–219.

E.Richard and S.Scavarda, 1989. "Non-linear control of a pneumatic servodrive", *Bath Int. Fluid Power Workshop,*, Vol. , pp. 59–74.

F.Xiang and J.Wikander, 2004. "Block-oriented approximate feedback linearization for control of pneumatic actuator system", *Control Engineering Practice*, Vol. **12**, no. 4, pp. 387–399.

Hung, J., 1993. "Chattering handling for variable structure control systems", *Industrial Electronics, Control, and Instrumentation*, Vol. **2**, pp. 1968–1972.

Hung, J. Y., Gao, W., and Hung, J. C., 1993. "Variable structure control: A survey", *IEEE Transactions on Industrial Electronics*, Vol. **40**, no. 1.

J.Wang, J.Pu, and P.Moore, 1999. "A practical control strategy for servo-pneumatic actuator systems", *Control Engineering Practice*, Vol. **7**, no. 12, pp. 1483–1488.

Kaasa, G.-O., 2003. *Nonlinear output-feedback control applied to electro-pneumatic clutch actuation in heavy-duty trucks*. PhD thesis, NTNU.

Khalil, H. K., 2000. *Nonlinear Control*. Pearson Education International. ISBN 0131227408.

Kimura, T., Hara, S., Fujita, T., and Kagawa, T., 1997. "Feedback linearization for pneumatic actuator systems with static friction", *Control Engineering Practice*, Vol. **5**, no. 10, pp. 1385–1394.

Koshkouei, A., Burnham, K., and Zinober, A., 2005. "Dynamic sliding mode control design", *Control Theory and Applications, IEE Proceedings*, Vol. **152**, no. 4, pp. 392–396.

Laghrouche, S., Smaoui, M., and Plestan, F., 2004. "Robust control of electropneumatic actuator by 3rd-order sliding mode", *43rd IEEE Conference on Decision and Control*, Vol. **4**, pp. 4375–4380.

Lagrouch, S., Smaoui, M., Plestan, F., and Brun, X., 2006. "Higher order sliding mode control based on optimal approach of an electropneumatic actuator", *International Journal of Control*, Vol. **79**, no. 2, pp. 119131.

Levant, A., 1998. "Robust exact differentiation via sliding mode technique", *Automatica*, Vol. **34**, no. 3, pp. 379–384.

Levant, A., 2003. "Higher-order sliding modes, differentiation and output-feedback control", *International Journal of Control*, Vol. **76**, no. 9-10, pp. 924–941.

Lokken, K., 2006. "Adaptive backstepping with application with electro-pneumatic clutch actuators". Master's thesis, NTNU.

Pandian, S. R., Hayakawa, Y., Kanazawa, Y., Kamoyama, Y., and Kawamura, S., 1997a. "Practical design of a sliding mode controller for pneumatic actuators", *Journal of dynamic systems, measurement, and control*, Vol. **119**, no. 4, pp. 666–674.

Pandian, S. R., Hayakawa, Y., Kanazawa, Y., Kamoyama, Y., and Kawamura, S., 1997b. "Practical design of adaptive model-based sliding mode control ofpneumatic actuators", *IEEE/ASME International Conference on Advanced Intelligent Mechatronics*, Vol. , pp. 140–.

Paul, A. K., Mishra, J. K., and Radke, M. G., 1994. "Reduced order sliding mode control for pneumatic actuator", *IEEE Transactions on control systems technology*, Vol. **2**, no. 3.

Shih, M. and Huang, Y., 1992. "Pneumatic servo-cylinder position control using a self-tuning controller", *JSME international journal*, Vol. **35**, no. 2, pp. 247254.

Slotine, J.-J. E. and Li, W., 1991. *Applied Nonlinear Control*. Prentice-Hall.

T.Acarman, C.Hatipoglu, and U.Ozguner, 2001. "A robust nonlinear controller design for a pneumatic actuator", *Proceedings of the 2001 American Control Conference*, Vol. **6**, pp. 4490–4495.

Utkin, V. I., 1977. "Variable structure systems with sliding modes", *IEEE Transactions on Automatic Control*, Vol. **22**, no. 2.

Vallevik, G. O., 2006. "Adaptive nonlinear observer for electropneumatic clutch actuation". Master's thesis, NTNU.

Virvalo, T., 1995. *Modelling and Design of a Pneumatic Position Servo System Realized with Commercial Components.* PhD thesis, Tampere University of Technology,.

X.Brun, M.Belgharbi, S.Sesmat, D.Thomasset, and S.Scavarda, 1999. "Control of an electropneumatic actuator: comparison between some linear and non-linear control laws", *Proceedings of the Institution of Mechanical Engineers, Part I: Journal of Systems and Control Engineering*, Vol. **213**, no. 5, pp. 387–406.

Young, K. D., 2002. "A control engineers guide to sliding mode control", *IEEE Transactions on Control System Technology*, Vol. **7**, no. 3, pp. 328–342.

APPENDIX A

MATHEMATICAL RESULTS

In this Appendix some mathematical results are presented, including

- Details of the simulation model
- Table of parameters used in the simulation model
- Conversion to normal form of the simple design model
- Details of the stability analysis of the ideal, boundary layer and integral controller

A.1 SIMULATION MODEL

A.1.1 PRESSURE AND TEMPERATURE

As Lokken (2006) and Kaasa (2003) describes the pressure and temperature in the two chambers are described by the following dynamic models

$$\begin{aligned}
\dot{p}_A =& -\frac{\kappa A_A v}{V_A(y)} p_A + \frac{\kappa R T_{in,A}}{V_A(y)} w_{in,A} + \frac{\kappa R T_A}{V_A(y)} w_{out,A} + \frac{(\kappa-1) H_w A_{w,A}(y)}{V_A(y)} (T_w - T_A) \\
\dot{T}_A =& -\frac{(\kappa-1) A_A v}{V_A(y)} T_A + \frac{(\kappa T_{in,A} - T_A) R T_A}{p_A V_A(y)} w_{in,A} \\
& - \frac{(\kappa-1) R {T_A}^2}{p_A V_A(y)} w_{out,A} + \frac{(\kappa-1) T_A H_w A_{w,A}(y)}{p_A V_A(y)} (T_w - T_A) \\
\dot{p}_B =& -\frac{\kappa A_B v}{V_B(y)} p_B + \frac{\kappa R T_{in,B}}{V_B(y)} w_{in,B} + \frac{\kappa R T_B}{V_B(y)} w_{out,B} + \frac{(\kappa-1) H_w A_{w,B}(y)}{V_B(y)} (T_w - T_B) \\
\dot{T}_B =& -\frac{(\kappa-1) A_B v}{V_B(y)} T_B + \frac{(\kappa T_{in,B} - T_B) R T_B}{p_B V_B(y)} w_{in,B} \\
& - \frac{(\kappa-1) R {T_B}^2}{p_B V_B(y)} w_{out,B} + \frac{(\kappa-1) T_B H_w A_{w,B}(y)}{p_B V_B(y)} (T_w - T_B)
\end{aligned}$$

where p_A and p_B describes the pressure in the two chambers A and B, while T_A and T_B represent the temeperatures. The air is considered an ideal gas, with κ as the ratio of spesific heat and R as the gas constant. $T_{in,A}$ and $T_{in,B}$ are the tempereatures of the

air flowing into chambers A and B. T_w is the temperature of the actuator cylinder wall, while H_w is the empirical convective heat coefficient. $V_A(y)$ and $V_B(y)$ are the volumes of the two chambers and $A_{w,B}(y)$ and $A_{w,B}(y)$ represent the effective wall area of heat transfer. They are given by the following equation

$$\begin{aligned} V_A(y) &= V_{A,0} + A_A y \\ A_{w,A}(y) &= A_{w,A_0} + L_w y \\ V_B(y) &= V_{B,0} + A_B y \\ A_{w,B}(y) &= A_{w,B_0} + L_w y \end{aligned}$$

where A_A and A_B are the areas of the chambers. $V_{A,0}$ and A_{w,A_0} represent the values of $V_A(y)$ and $A_{w,A}$ when $y = 0$ respectively, and the same for chamber B. L_w is the inner perimeter of the cylinder wall.

A.1.2 Chamber A: Flow and valve modeling

For a single valve the steady-state flow rate is given by

$$w_v = q_v(p_h, p_l, u_v, C, B, \Theta_v) = g_v(p_h, p_l, u_v, C, B) \cdot y_v(u_v, \Theta_v) \tag{A.1}$$

where the flow capacity, $g_v(p_h, p_l, u_v, C, B)$ is given as

$$g_v(p_h, p_l, u_v, C, B) = \rho_0 C \psi\left(\frac{p_l}{p_h}, B\right) p_h, \quad p_h \geq p_l$$

A multi-regime pressure ratio function is used

$$\psi(r, B) \equiv \psi_0(r, 0) + B \begin{cases} \psi_0(r, B^*) - \psi_0(r, 0) & , \quad B \geq 0 \\ \psi_0(r, 0) + r - 1 & , \quad B < 0 \end{cases}, \quad r \in [0, 1]$$

where $B^* = 0.528$ is the critical pressure ratio function and the nominal pressure ratio function is given by

$$\psi_0(r, B_0) \equiv \begin{cases} 1 & , \quad r < B_0 \\ \sqrt{1 - \left(\frac{r - B_0}{1 - B_0}\right)^2} & , \quad r \leq B_0 \end{cases}$$

The normalized valve opening y_v can be parametrized in various forms, and a general representation for these are

$$y_v = h_v(u_v, \Theta_v)$$

where u_v is the duty cycle of the valve's PWM input and Θ_v is a parameter vector.

In the model used for the simulation model in this thesis, a look-up table with linear interpolation is used to paramtrize the PWM characteristic, $h_v(u_v, \Theta_v)$. The vectors in the look-up table is defined as follows

$$\mathbf{u}_{v,char} = [0, R_{0,lb}, R_{0,ub}, R_1]$$
$$\mathbf{y}_{v,char} = [0, \Theta_{v,0}, \Theta_{v,1}, 1]$$

To find the complete flow model of chamber A the following relation is used

$$w_v = w_{v,in} - w_{v,out}$$

Combined with the previous results this yields the following flow model for chamber A

$$\begin{aligned} w_v &= g_{v,in}(p_s, p_A, u_{vs}, C_{vs}, B_{vs}) \cdot y_{vs}(u_{vs}, \Theta_{vs}) - g_{v,out}(p_A, p_E, u_{ve}, C_{ve}, B_{ve}) \cdot y_{ve}(u_{ve}, \Theta_{ve}) \\ &= \rho_0 C_{vs} \psi \left(\frac{p_A}{p_s}, B_{vs} \right) p_s y_{vs}(u_{vs}, \Theta_{vs}) - \rho_0 C_{ve} \psi \left(\frac{p_E}{p_A}, B_{ve} \right) p_A y_{ve}(u_{ve}, \Theta_{ve}) \end{aligned}$$

A.1.3 Chamber B: Flow model

The flow through the actuator restriction of chamber B is modelled in the same fashion as in (Lokken, 2006)

$$w_r = w_{r,in} - w_{r,out} \quad = \rho_0 \sqrt{T_0} C_r \cdot \omega_r \left(\frac{p_B}{P_E} \right) \frac{p_E}{\sqrt{T_E}} - \rho_0 \sqrt{T_0} C_r \cdot \omega_r \left(\frac{p_E}{P_B} \right) \frac{p_B}{\sqrt{T_B}}$$

where $w_{r,in}$ and $w_{r,out}$ describes the flow in and out of chamber B respectively. C_r is the flow conductance for the restriction, p_E and T_E are the pressure and temperature outside the exhaust restriction.

The flow rate model for w_r are also the same as described by Lokken (2006) and is given by

$$\omega_r(r) = \Omega_0(r) + b_r \cdot \Omega_1(r, sgn(b_a)), \quad b_a \in [-1, 1]$$

where r describes the ratio between low and high pressure, $r = \frac{p_l}{p_h}$. The functions $\Omega_0(r)$ og $\Omega_1(r, sgn(b_a))$ are defined as

$$\Omega_0(r) = \begin{cases} \sqrt{1 - r^2}, & r \in [0, 1] \\ 0, & r > 1 \end{cases}$$

$$\Omega_1(r, +1) = -\Omega_0(r) + \begin{cases} 1, & r \in [0, B_0] \\ \sqrt{1 - \left(\frac{r - B_0}{1 - B_0} \right)^2}, & r \in \langle B_0, 1] \\ 0, & r > 1 \end{cases}$$

$$\Omega_1(r,-1) = \Omega_0(r) - \begin{cases} 1-r, & r \in [0,1] \\ 0, & r > 1 \end{cases}$$

where B_0 is the critical pressure ratio.

A.1.4 Simulation model parameters

The table below show the parameters used in the simulation model

Parameter	Value	Unit	Description
Reference values			
T_0	293	K	Enviromental temperature
P_0	10^5	Pa	Enviromental pressure
P_E	P_0	Pa	Exhaust pressure
P_s	$9.5 \cdot 10^5$	Pa	Supply pressure
R	288	$\frac{J}{K \cdot kg}$	Gas constant of air
ρ_0	1.185	$\frac{kg}{m^3}$	Air density
Clutch actuator			
A_A	$12.3 \cdot 10^-3$	m	Area of chamber A
A_B	A_A	m	Area of chamber B
$V_{A,0}$	$0.8 \cdot 10^-3$	m^3	Volume of chamber A at y = 0
$V_{B,0}$	$0.57 \cdot 10^-3$	m^3	Volume of chamber B at y = 0
M	10	kg	Mass of the piston
Flow parameters			
B_0	0.528	-	Critical pressure ratio
C_r	$2.1173 \cdot 10^-8$	$\frac{m^3}{Pa \cdot s}$	Flow conductance of the exhaust restriction
b_r	-0.7596	-	Parameter in the flow rate model of chamber B
Valve parameters			
C_{vs}	$7.7 \cdot 10^-9$	-	Flow conductance for supply valve
C_{ve}	$9.2 \cdot 10^-9$	-	Flow conductance for exhaust valve
B_{vs}	0.6	-	Critical pressure ratio of supply valve
B_{ve}	-0.8	-	Critical pressure ratio of exhaust valve
Friction parameters			
α_l	$3.07 \cdot 10^3$	m^2	-

D_v	$1.39 \cdot 10^3$	$\frac{N \cdot s}{m}$	Viscous damping coefficient
K_f	$3.26 \cdot 10^4$	$\frac{N}{m}$	Deflection stiffness
D_f	$1.14 \cdot 10^2$	$\frac{N \cdot s}{m}$	Deflection damping coefficient
F_C	$1.72 \cdot 10^2$	N	Coloumb friction level
F_S	$3.52 \cdot 10^2$	N	Stiction force level
v_s	0.2254	$\frac{m}{s}$	Striebeck velocity

Temperatur and air dynamics parameters

L_w	$2 \cdot \sqrt{\pi \cdot A_A}$	m	Inner perimeter in actuator
κ	1.4	-	-
A_{w,A_0}	0.078	m^2	Value of $A_{w,A}$ at y = 0
A_{w,B_0}	$1.00 \cdot 10^-4$	m^2	Value of $A_{w,A}$ at y = 0
H_w	10.16	$\frac{W}{m^2 \cdot K}$	Empirical convective heat coefficient
T_w	293	K	Temperature of cylinder wall

A.2.1 NORMAL FORM OF SIMPLIFIED CONTROL MODEL

For the model in 3.9

$$h(x) = y \text{ and } \rho = 3$$

Thus

$$\begin{aligned}
\psi_1(\mathbf{x}) &= h(\mathbf{x}) = y \\
\psi_2(\mathbf{x}) &= L_f h(\mathbf{x}) = \frac{\delta y}{\delta \mathbf{x}} = \begin{bmatrix} 1 & 0 & 0 \end{bmatrix} f(\mathbf{x}) = v \\
\psi_3(\mathbf{x}) &= L_f^2 h(\mathbf{x}) = \frac{\delta v}{\delta \mathbf{x}} = \begin{bmatrix} 0 & 1 & 0 \end{bmatrix} f(\mathbf{x}) \\
&= \frac{1}{M}\left[-f_l(y) - f_f(v) + A(p - P_0)\right]
\end{aligned}$$

The new normal form state system is given by

$$\begin{aligned}
\dot{\xi_1} &= \xi_2 \\
\dot{\xi_2} &= \xi_3 \\
\dot{\xi_3} &= f(\boldsymbol{\xi}) + g(\boldsymbol{\xi})u
\end{aligned} \tag{A.2}$$

The expressions for $f(\boldsymbol{\xi})$ and $g(\boldsymbol{\xi})$ are found from

$$\begin{aligned}
\frac{d}{dt}\xi_3 &= \frac{d}{dt}\psi_2(\mathbf{x}) \\
&= \frac{d}{dt}\frac{1}{M}\left[-f_l(y) - f_f(v) + A(p - P_0)\right] \\
&= \frac{1}{M}\left[-\frac{d}{dt}f_l(\xi_1) - \frac{d}{dt}f_f(\xi_2) + A\dot{p}(\boldsymbol{\xi})\right]
\end{aligned} \tag{A.3}$$

where

$$\begin{aligned}
\frac{d}{dt}f_l(\xi_1) &= K_l L_l \xi_2 e^{-L_l \xi_1} - M_l \xi_2 \\
\frac{d}{dt}f_f(\xi_2) &= D\xi_3 \\
p(\boldsymbol{\xi}) &= \frac{1}{A}\left[M\xi_3 + f_l(\xi_1) + f_f(\xi_2)\right] + P_0 \\
\dot{p}(\boldsymbol{\xi}) &= \frac{1}{V(\xi_1)}\left(-A\xi_2 p + RT_0 u\right)
\end{aligned} \tag{A.4}$$

Inserting A.4 into A.3 yields the expressions

$$f(\boldsymbol{\xi}) = -\frac{1}{M}\left[\frac{A}{V(\xi)}\xi_2\left(M\xi_3 + K_l(1-e^{-L_l\xi_1}) - M_l\xi_1 + D\xi_2 + AP_0\right)\right] + \frac{1}{M}\left[-K_lL_l\xi_2e^{-L_l\xi_1} + M_l\xi_2 - D\xi_3\right] \tag{A.5}$$

$$g(\boldsymbol{\xi}) = \frac{ART_0}{MV(\xi_1)} \tag{A.6}$$

A.3 Stability analysis

A.3.1 Ideal controller

Proof A.1 (Proof of equation 4.8)**.** *Suppose that the scalar differential equation*

$$\dot{s} = f_s(x), \quad s(0) = s_0$$

has a unique solution on $[0, t_1)$ *for some* $t_1 > 0$ *and* $f(x)$ *is locally Lipscithz. Given* $V = \frac{1}{2}s^2$*, and choosing* $W = \sqrt{2V} = |s|$ *then*

$$\dot{W} = \frac{d}{dt}\sqrt{2V} = 2\dot{V}\frac{1}{2\sqrt{2V}} = \frac{\dot{V}}{\sqrt{2v}} = \frac{\dot{V}}{|s|}$$
$$D^+W \leq -G_0\beta_0$$

Letting W_0 *be the solution to the differential solution*

$$\dot{W}_0 = -G_0\beta_0, \quad W_0(0) = |s(0)|$$

then

$$W_0(t) = \int_0^T -G_0\beta_0 dt$$
$$W_0(t) = W_0(0) - G_0\beta_0 t$$

then by the comparison lemma

$$W(t) \leq W_0(0) - G_0\beta_0 t$$

and since $W = |s|$

$$|s(t)| \leq |s(0)| - G_0\beta_0 t \quad \square$$

Proof A.2 (Proof of equation 4.11)**.** *Given that $s\dot{s} \leq 0$ in the set $\{|s| \leq \epsilon\}$, and the linear system*

$$\begin{aligned}\dot{e_1} &= e_2 \\ \dot{e_2} &= -a_2 e_2 - a_1 e_1 + s\end{aligned}$$

where $e = e_1, \dot{e} = e_2$ and $\boldsymbol{e} = [e_1\ e_2]^T$. Choosing the Lyapunov function

$$\begin{aligned}V_1(\boldsymbol{e}) &= \frac{1}{2}\boldsymbol{e}^T P \boldsymbol{e} \\ &= \frac{1}{2}\begin{bmatrix} e_1 & e_2 \end{bmatrix}\begin{bmatrix} 2 & \frac{1}{a_2} \\ \frac{1}{a_2} & \frac{1}{a_1} \end{bmatrix}\begin{bmatrix} e_1 \\ e_2 \end{bmatrix} \\ &= \frac{1}{2}(2e_1^2 + \frac{2}{a_2}e_1 e_2 + \frac{1}{a_1}e_2^2) \\ &= e_1^2 + \frac{1}{a_2}e_1 e_2 + \frac{1}{2a_1}e_2^2\end{aligned}$$

The time-derivative of V is then given as

$$\begin{aligned}\dot{V}_1(\boldsymbol{e}) &= -\frac{a_1}{a_2}e_1^2 - \frac{a_2^2 - a_1}{a_1 a_2}e_2^2 + \frac{1}{a_2}e_1 s + \frac{2}{a_1}e_2 s \\ &\leq -\frac{a_1}{a_2}e_1^2 - \frac{a_2^2 - a_1}{a_1 a_2}e_2^2 + \frac{\epsilon}{a_2}|e_1| + \frac{\epsilon}{a_1}|e_2|\end{aligned}$$

To prove stability of the system the following conditions must hold for the Lyapunov function candidate

$$\begin{aligned}&1)\ V_1(\boldsymbol{e}) > 0,\ \forall \boldsymbol{e} \neq 0 \\ &2)\ V_1(\boldsymbol{e}) = 0,\ \boldsymbol{e} = 0 \\ &3)\ V_1(\boldsymbol{e}) \to \infty,\ \|\boldsymbol{e}\| \to \infty \\ &4)\ \dot{V_1}(\boldsymbol{e}) \leq 0\end{aligned}$$

The first three conditions are satisfied if the matrix P is positive definite, which will be the case if the leading principle minors are positive. This gives the following inequalities

$$\begin{aligned}&1)\ 2 > 0 \\ &2)\ a_2 > \sqrt{\frac{a_1}{2}}\end{aligned}$$

To achieve $\dot{V} \leq 0$ the following inequalities must hold

$$\begin{aligned} |e_1| &\geq \frac{\epsilon}{a_1} \\ |e_2| &\geq \frac{\epsilon a_2}{a_2^2 - a_1} \\ a_2 &> \sqrt{a_1} \end{aligned}$$

Thus, by the comparison lemma

$$\begin{aligned} |e_1(0)| \leq \frac{\epsilon}{a_1} \Rightarrow |e_1(t)| \leq \frac{\epsilon}{a_1}, \quad \forall t \geq 0 \\ |e_2(0)| \leq \frac{\epsilon}{a_2 - 2} \Rightarrow |e_2(t)| \leq \frac{\epsilon a_2}{a_2^2 - a_1}, \quad \forall t \geq 0 \end{aligned}$$

and the set

$$\Omega_\epsilon = \left\{ |e_1| \leq \frac{\epsilon}{a_1}, |e_2| \leq \frac{\epsilon a_2}{a_2^2 - a_1}, |s| \leq \epsilon \right\}$$

is positively invariant.

Proof A.3. *Inside Ω_ϵ the input u is reduced to*

$$u = u_{eq} - k\frac{s}{\epsilon} = u_{eq} - \frac{k}{\epsilon}(e_3 + a_2 e_2 + a_1 e_1)$$

The closed-loop system is then given by

$$\begin{aligned} \dot{e_1} &= e_2 (= f_1) \\ \dot{e_2} &= e_3 (= f_2) \\ \dot{e_3} &= f(\boldsymbol{\xi}) - \dddot{r} + g(\boldsymbol{\xi}) \left[u_{eq} - \frac{k}{\epsilon}(e_3 + a_2 e_2 + a_1 e_1) \right] (= f_3) \end{aligned} \tag{A.7}$$

Then, by setting $\dot{e}_1 = \dot{e}_2 = \dot{e}_3 = 0$

$$\begin{aligned} \bar{e_2} = 0 \quad &\Rightarrow \quad \bar{\xi_2} = \bar{v} = \dot{r} \\ \bar{e_3} = 0 \quad &\Rightarrow \quad \bar{\xi_3} = \dot{\bar{v}} = \ddot{r} \\ \bar{e_1} &= \frac{\epsilon(f(\hat{\boldsymbol{\xi}} - \hat{f}(\hat{\boldsymbol{\xi}})}{k a_1 g(\hat{\boldsymbol{\xi}}))} \end{aligned}$$

The closed loop system in A.7 then has an equilibrium point $\bar{\boldsymbol{e}} = [\bar{e_1}\ 0\ 0]$

For simplicity only a constant refernce is considered in this theis, thus

$$r = c \quad \Rightarrow \quad \dot{r} = \ddot{r} = \dddot{r} = 0$$

The assumptions above means that the system in A.7 has a unique equilibrium point in $\bar{\boldsymbol{e}} = [0\ 0\ 0]^T \Rightarrow \bar{y} = c, \bar{v} = 0, \dot{\bar{v}} = 0$. *Since the set* Ω_ϵ *is positively invariant all trajectories converge to this set and therefore only a local stability analysis is performed. As described in Section 2.3 in (Khalil, 2000) the qualitative behaviour near an equilibrium point can be approximated through a linearization around the equilibrium point. First a new set of variables are defined*

$$\Delta \boldsymbol{e} = \begin{bmatrix} \Delta e_1 \\ \Delta e_2 \\ \Delta e_3 \end{bmatrix} = \begin{bmatrix} e_1 - \bar{e_1} \\ e_2 - \bar{e_2} \\ e_3 - \bar{e_3} \end{bmatrix}$$

The linerazed model aroud $\bar{\boldsymbol{e}}$ *can the be written as*

$$\Delta \dot{\boldsymbol{e}} = A_\delta \Delta \boldsymbol{e} = \begin{bmatrix} a_{11}\ a_{12}\ a_{13} \\ a_{21}\ a_{22}\ a_{23} \\ a_{31}\ a_{32}\ a_{33} \end{bmatrix} \Delta \boldsymbol{e}$$

where A_δ *is the linerized system Matrix defined as*

$$A_\delta = \begin{bmatrix} \frac{\partial f_1}{\partial e_1} & \frac{\partial f_1}{\partial e_2} & \frac{\partial f_1}{\partial e_3} \\ \frac{\partial f_2}{\partial e_1} & \frac{\partial f_2}{\partial e_2} & \frac{\partial f_2}{\partial e_3} \\ \frac{\partial f_3}{\partial e_1} & \frac{\partial f_3}{\partial e_2} & \frac{\partial f_3}{\partial e_3} \end{bmatrix}_{e=\bar{e}} \tag{A.8}$$

where f_1, f_2 *and* f_3 *are found from A.7. After some calculations the following expressions are found for the elements of* A_δ

$$\begin{aligned} a_{11} &= 0,\ a_{12} = 1,\ a_{13} = 0 \\ a_{21} &= 0,\ a_{22} = 0,\ a_{23} = 1 \\ a_{31} &= \frac{k \cdot a_1}{\epsilon} \left[\frac{cA^2 RT_0}{M \cdot (V_0 + Ac)^2} - \frac{ART_0}{M \cdot (V_0 + Ac)} \right] \\ a_{32} &= -\frac{k \cdot a_2}{\epsilon} g(\boldsymbol{\xi}) \\ a_{33} &= -\frac{k}{\epsilon} g(\boldsymbol{\xi}) \end{aligned}$$

For simplicity it is assumed in the expressions above that the equivalent control law cancels out all the non-linearities perfectly (u_{eq} = $f(\boldsymbol{\xi})$).

A.3.3 CONTROLLER WITH INTEGRAL EFFECT

Given a Lyapunov-like function $V(s) = \frac{1}{2}s^2$ and the sliding surface $s(\mathbf{e}) = a_0e_0 + a_1e_1 + a_2e_2 + e_3$ the following result is obtained

$$\begin{aligned}\dot{V} &= s\dot{s} \\ &= s[f(\boldsymbol{\xi}) + a_2e_3 + a_1e_2 + a_0e_1 - \dddot{r} + g(\boldsymbol{\xi})u]\end{aligned}$$

then by choosing the equivalent control law

$$u_{eq} = \frac{1}{g(\boldsymbol{\xi})}\left[-\hat{f}(\boldsymbol{\xi}) - a_2e_3 - a_1e_2 - a_0e_1 + \dddot{r}\right] \tag{A.9}$$

the analysis of the system in the reaching phase will be equivalent to the analysis in Section 4.1.

The motion on the sliding surface is goverened by

$$e_3 = -a_2e_2 - a_1e_1 - a_0e_0 \tag{A.10}$$

which means $e(t)$ will converge to zero once the sliding surface, S is reached. The rest of the stability analysis will also corespond to Section 4.1 and therefore the SMC with integral effect will render the system globally asymptotically stable.

PLOTS FROM SIMULATIONS AND EXPERIMENTS

B.1 CONTROLLER IMPROVEMENTS SIMULATIONS

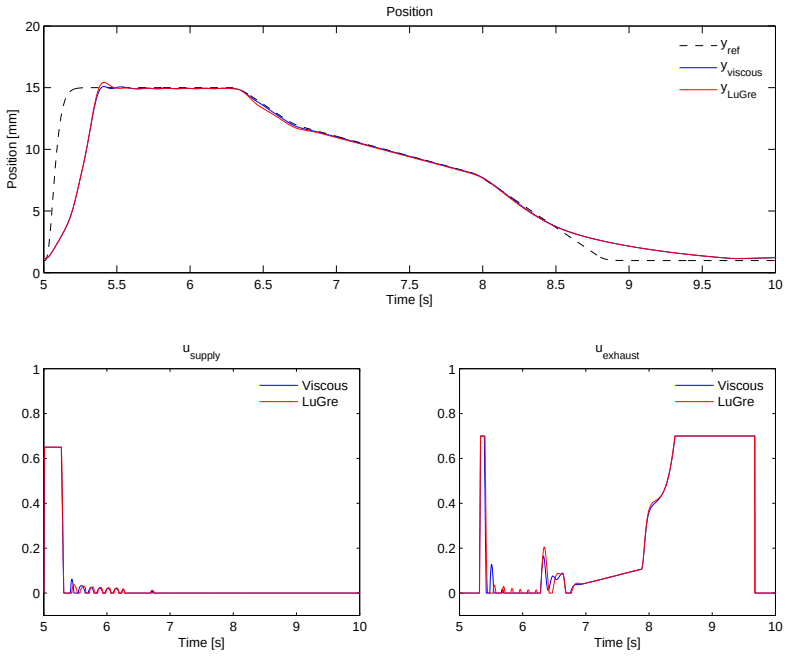

Figure B.1: Comparison between controller performance with viscous and LuGre friction models

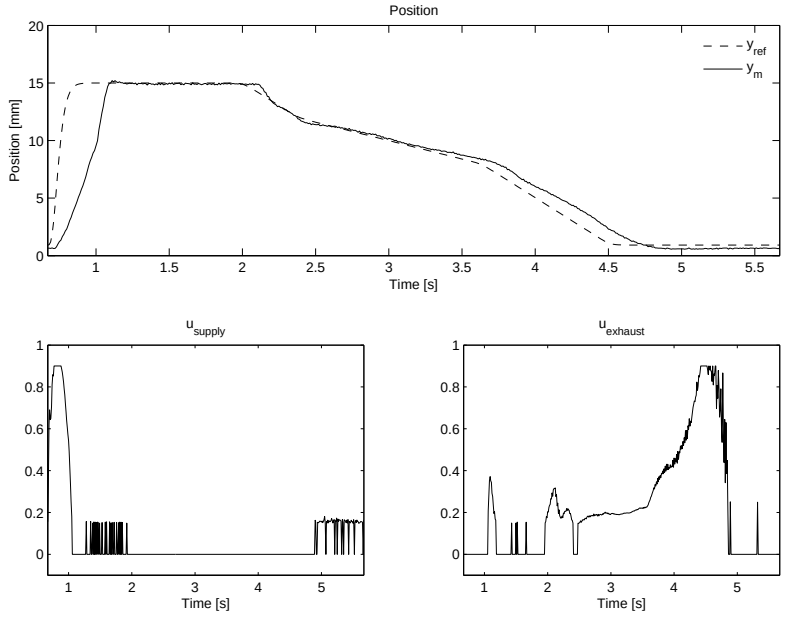

Figure B.2: Case 1: Nominal values in the controller

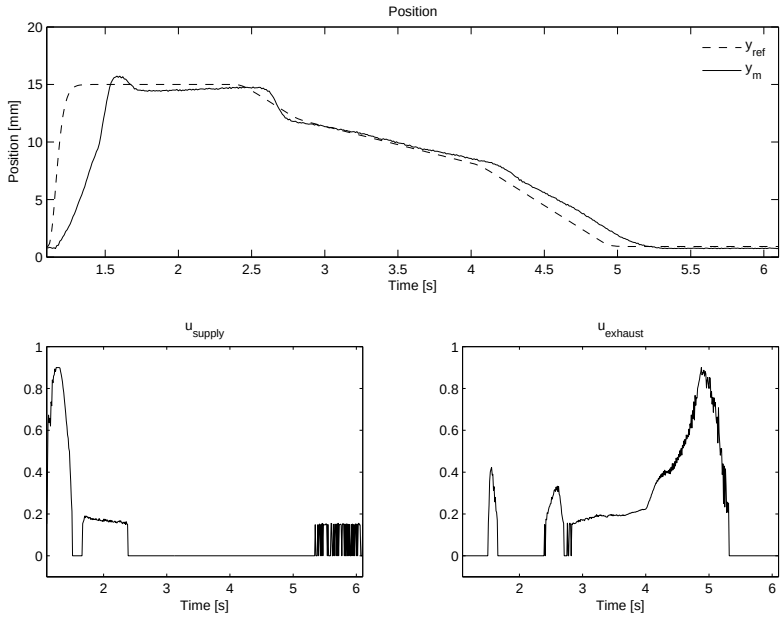

Figure B.3: Case 2: Load characteristic lowered 1000N in the controller compared to the nominal values

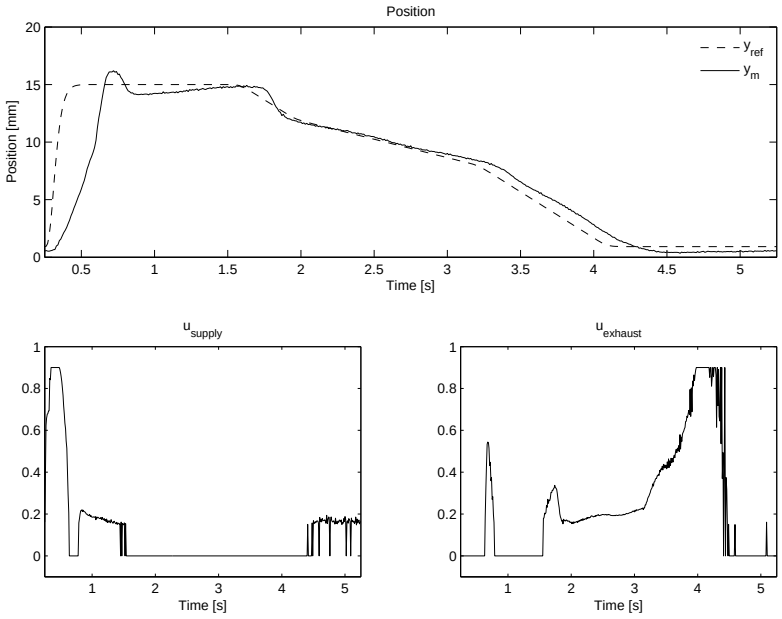

Figure B.4: Case 3: Load characteristic raised 1000N in the controller compared to the nominal values

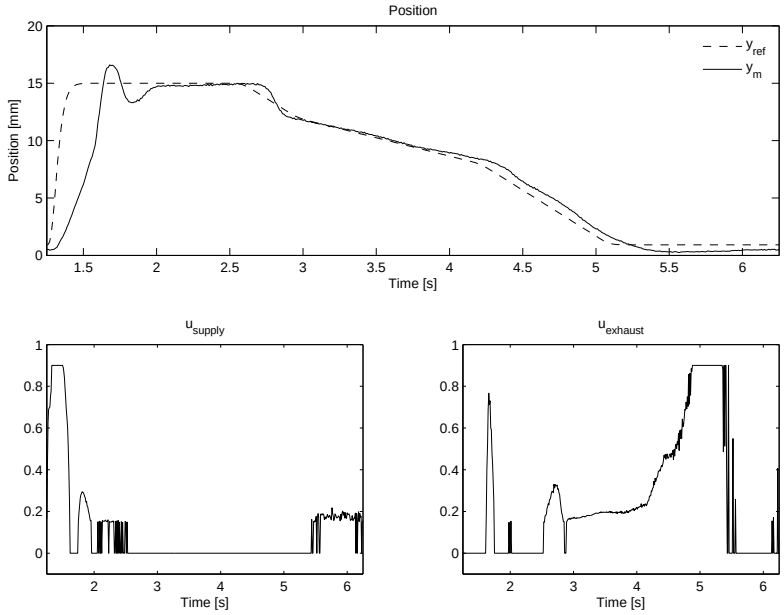

Figure B.5: Case 4: Load characteristic raised 1000N in the controller compared to the nominal values AND initial volume increased by 50%

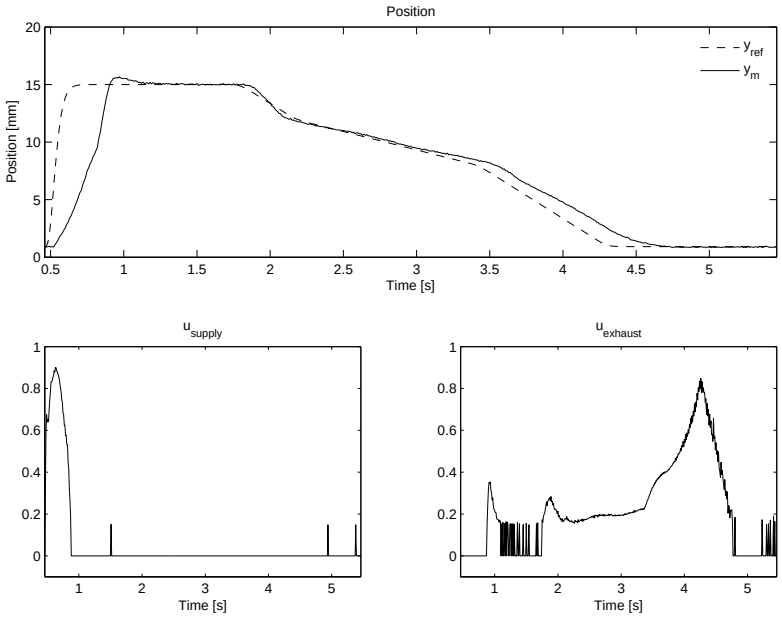

Figure B.6: Case 5: Load characteristic raised 1000N in the controller compared to the nominal values AND initial volume decreased by 50%

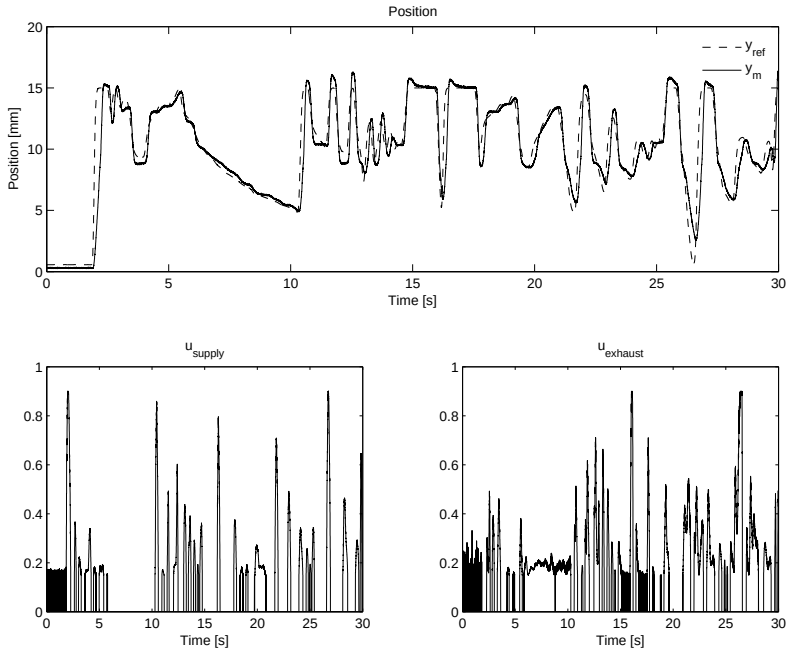

Figure B.7: Random reference tested with Sliding Mode Controller

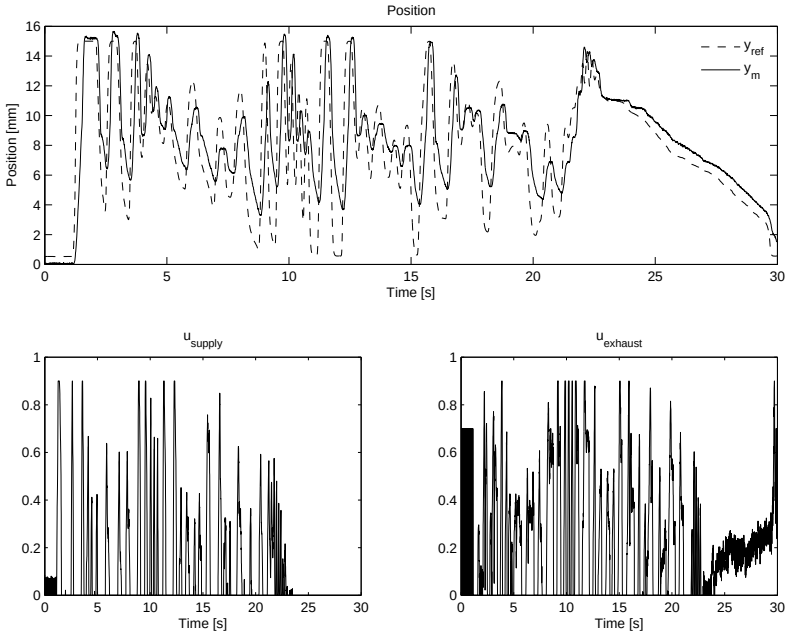

Figure B.8: Random reference tested with PD controller

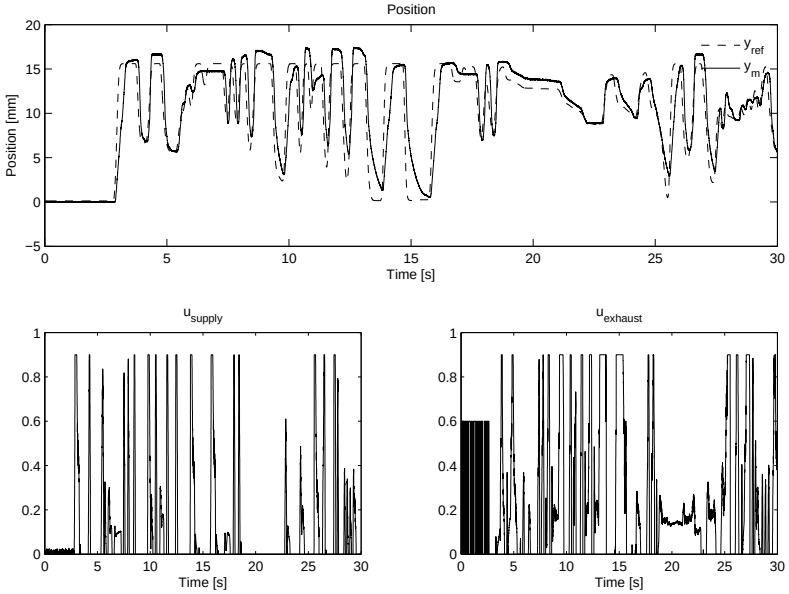

Figure B.9: Random reference tested with Backstepping controller